CHEMICAL INTERACTIONS BETWEEN POLYCYCLIC AROMATIC HYDROCARBONS (PAHs) AND SEDIMENTS: INTERACTION OF NAPHTHALENE WITH MARINE SEDIMENTS

by

NIDIA PATRICIA GRANADOS SAAVEDRA, B.Sc.

A thesis submitted to the

Chemistry Department and the Faculty of Graduate Studies and Research

in partial fulfillment of the requirements for the degree of

Master of Science in Applied Science

Saint Mary's University

Halifax, Nova Scotia, Canada

18 January 2004

Certification

Name: Nidia Patricia Granados S.

Degree: Master of Science

Title Thesis: Chemical Interactions Between Polycyclic Aromatic Hydrocarbons (PAHs) and Sediments: Interaction of Naphthalene with Marine Sediments

Examining Committee:

Dr. Stephen Duffy, External Examiner, Department of Chemistry, Mount Allison University, St. John's, Newfoundland

Dr. Marc M. Lamoureux , Co-Supervisor

Dr. Donald Gamble, Co-supervisor

Dr. Robert Singer, Supervisory Committee

Dr. Ron Russell, Supervisory Committee

Dr. William E. Jones, Acting Dean of Graduate Studies

Dr. David H. S. Richardson, Dean of Science

Date Certified: February 26, 2004

In memory of my father…Pedro León ...

ABSTRACT

Nidia Patricia Granados S.

Chemical Interactions Between Polycyclic Aromatic Hydrocarbons (PAHs) and Sediments: Interaction of Naphthalene with Marine Sediments

January 18 2004

A methodology for studying sorption kinetics of naphthalene in sediments and, for monitoring the free and sorbed forms of naphthalene, has been developed using High Performance Liquid Chromatography online microextraction and offline phase separation methodologies. Investigations of naphthalene sorption in two marine sediments were carried out at 25 ºC to assess the suitability of the method for volatile analytes. Results of sorption kinetics are consistent with a two-step process in which the first step involves labile sorption of naphthalene onto the sediment. In the second step, naphthalene becomes unrecoverable. Pseudo-first order rate coefficients for the disappearance of naphthalene from solution were obtained in the order of 90 day^{-1} for an initial fast sorption step and 0.5 day^{-1} for a slower sorption step.

ACKNOWLEDGEMENTS

This thesis could not have been accomplished without the support of many people. I wish to express my deep gratitude to my supervisors Dr. Marc Lamoureux and Dr. Donald Gamble for opening this extraordinary research opportunity to me, for providing me with the bases to address this challenged project and for their guidance and support. I am greatly indebted to Dr. Kathy Singfield for her help during the early stages of writing this thesis, and for her encouragement and willingness to entrust the presentation of this project. I would like to thank also Dr William Bridgeo for his suggestions to improve the third endless chapter.

I wish to thank all the people in the laboratory, my lab mates for their friendship and the students who took part at some point in this project, especially to Melissa Laundry, Sarah Stockley, Tanya Hutchinson and Monika Skalski. Thanks are due also to Elizabeth McLeod and Darlene Goucher for their assistance at all times with all types of technical problems I run into.

I am forever indebted to my lovely husband David Mantilla for his understanding, infinite patience and his absolute confidence in me when it was most required. Finally I would like to thank my family that even though is far away, has been always here, giving us all the affections.

TABLE OF CONTENTS

LIST OF TABLES

LIST OF FIGURES

LIST OF ABBREVIATIONS

PAH	Polycyclic aromatic hydrocarbons
HPLC	High performance liquid chromatography
PDA	Photo-diode array detector
ppb	Parts per billion
ICP	Inductively coupled plasma
MS	Mass spectrometry
LD	Limit of detection
RSD	Relative standard deviation
CNS	Carbon Nitrogen Sulphur
CHN	Carbon Hydrogen Nitrogen
APCI	Atmospheric-pressure chemical ionization
rpm	Revolutions per minute
PTFE	Polytetrafluoroethylene
UV	Ultraviolet

CHAPTER ONE

1 INTRODUCTION

1.1 Polycyclic Aromatic Compounds

Polycyclic aromatic compounds, (PAH) are persistent contaminants in the environment and their chemical and physical interactions with natural solids have been the focus of intense research for several decades. This interest is a result of their ubiquitous nature, their increasing anthropogenic loading in the environment and their potentially hazardous effects on nature. The formation, distribution, and importance of these compounds in the environment have been studied in detail. These three topics are briefly introduced in *Chapter One*. In addition, a review of some of the extensive analytical methods that have been developed to follow the kinetics of distribution of PAHs is presented.

PAHs are composed of two or more fused aromatic rings formed of carbon and hydrogen atoms, arranged in linear, angular or clustered rings. The chemical and physical properties of these compounds vary widely and are strongly dependant on the structure of the individual compound and its molecular weight. Two groups of PAHs can be distinguished on the basis of molecular weight. Low molecular weight PAHs are composed of two to three aromatic rings (e.g. naphthalene, fluorenes, phenanthrene, and anthracene) and high molecular weight PAHs are comprised of four to seven aromatic

rings (e.g. chrysene, and coronene). For example, naphthalene and chrysene have the following chemical structure:

Naphthalene $C_{10}H_8$ Chrysene $C_{18}H_{12}$

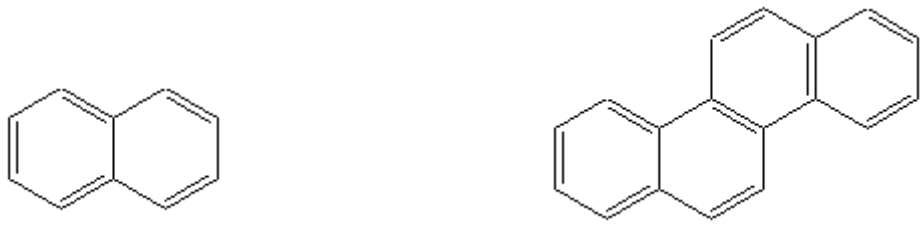

There exist some distinguishing trends among PAHs with molecular weight. With increasing molecular weight, resistance to oxidation and reduction tends to decrease, vapor pressure and aqueous solubility decrease almost logarithmically; and melting point and boiling point increase. [1]

The distribution and persistence of PAHs in the environment and their effects on biological systems also vary substantially with molecular weight. Low molecular weight PAHs are known to have significant acute toxicity to aquatic organisms whereas high molecular weights have been proven to be carcinogenic. [2]

1.2 Sources of PAH in the Aquatic Environment

PAHs may be formed by a variety of processes including high temperature pyrolysis of organic materials, low to moderate temperature diagenesis of sedimentary in the formation of fossil fuel, and direct biosynthesis by microbes and plants. [3]

Although the presence of PAHs can be attributed to natural processes, a wide variety of human activities increase the environmental load of these substances. Direct inputs of PAHs from oil spills, wastewaters, storm water and petrolysis tend to contribute to pollution in urban and industrial areas. Petroleum spills represent the major direct anthropological source of PAHs in oceans and devastating impacts on aquatic systems. For example, levels of PAH in sediments of pristine areas have been found in the range of 200 μg/kg to 500 μg/kg, and in heavily industrialized areas in the range of 10 000 μg/kg to several hundred thousand μg/kg. [2]

It is assumed that once PAH compounds enter the aquatic environment, a cycle of sorption-desorption starts. PAHs are sorbed by organic and inorganic particulate matter, which subsequently settles in sediments. Leaching or biological activity in the sediment may return a small fraction of sediment-PAH to the water column. Concentrations of PAH in aquatic systems are typically found to be relatively high in sediments, intermediate in aquatic biota, and low in the water column. Natural routes of removal of PAH from the aquatic environment include, volatilization, photoxidation, chemical oxidation, and microbiological metabolism. [2]

1.3 Interactions Between PAHs and Sediments

Interactions between hydrophobic organic compounds and sediments involve several processes, including physisorption/desorption, intraparticle diffusion, chemisorption, chemical and microbiological degradation.[4] Sorption is the process associated with the binding, migration and distribution of a compound in a solid. It is

identified as an important factor in the determination of the fate of hydrophobic molecules in water/sediment systems, controlling the concentration and rate of transport in aquifers, and potentially playing a significant role in controlling reactions that degrade organic chemicals. [5,6]

In the relevant context, the word *sorption* is a collective term referring to the general uptake of a substance by a sorbent and includes the two specific processes of *adsorption* and *absorption*. It is noteworthy to clarify these two terms. *Adsorption* is used to describe an uptake mechanism in which the adsorbed constituents are concentrated at the interface between two phases. The adsorbate is not transferred to the bulk phase of the adsorbent. Adsorption includes condensation onto a substrate from both solution and gas phase. The latter term, *absorption*, is used to depict the transfer of a component from the bulk state of one phase into the bulk state of another phase. [7]

Associated with the preceding concepts, the terms *sorbate* and *analyte* are used indistinguishably, throughout this document, to refer to the compound which sorption kinetics and distribution is measured. The terms *sorbent, substrate* or *geosorbent* are used to refer to the solid particles in which the sorbate is sorbed (i.e., sediment particles).

1.3.1 Interactions with Soil Organic Fraction

Sorption – desorption of hydrophobic organic compounds in soils and sediments has been described commonly as a process influenced by the chemical composition of the sorbent (i.e., nature of the organic matter content, and mineral composition), and in which the organic carbon content plays the main role in the sorption process of hydrophobic organic compounds.[8, 9]

The uptake of these nonionic compounds has been described as occurring by a partition sorption mechanism,[10] in which the sorbed organic chemical permeates into the bulk of the organic matter, is distributed homogeneously in the entire volume of the solid, and is retained by weak intermolecular forces (e.g., van der Waals London dispersion forces). In this sorption mechanism, the organic content of the sorbent is the 'solvent' for the sorbate. It resembles the mixing of two completely miscible liquids, in which there is no limits in the amount of sorbate that can be up taken by the organic matter.[10] In this concept, the sorption capacity of the solid, a fundamental property of sorbent, is neglected.

With this assumption, several approaches have been used in an attempt to describe and predict the distribution of the sorbate hydrophobic organic compounds in natural solids at equilibrium. For organic molecules taken up from solution onto a solid phase, a description of their equilibrium distribution between the solid and solution phases can be obtained using an empirical isotherm. Typically, the amount of sorbate molecules at equilibrium is measured both in solution and on solid phase sorbent, and this is repeated for solutions of different initial concentrations at constant temperature. The measurements are used to construct an isotherm, which can be described by, for example, the Freundlich isotherm equation:

$$\mathbf{C_s = K_f C_{aq}^{n}} \qquad \mathbf{(1.1)}$$

where C_s is the quantity of analyte sorbed per unit mass of sorbent (mol g^{-1}); C_{aq} is the equilibrium solution concentration (mol L^{-1}); and K_f (L g^{-1}) and n (a dimensionless number) are the empirical Freundlich constants. This equation does not imply any

particular mechanism of sorption and it has been found to satisfactorily describe sorption from solutions in the range of low initial sorbate molecule concentration, (i.e. < 1.0 M).[11]

For typical environmental pollutants concentrations in sediment suspensions, sorption isotherms approximate linearity, thus aqueous phase concentration is directly related to the sorbed pollutant concentration. Under these conditions, when the Freundlich constant, n, has a value of 1, the proportionality constant K_f becomes K_d (L g^{-1}), i.e., the distribution coefficient for the contaminant. Application of this equation has been valid for a narrow range of solute concentrations when partitioning is the only sorption mechanism.[12]

Karickhoff et al., describes the sorption of hydrophobic organic compounds, including some PAH in sediments, as a process controlled by the organic carbon content of the solid.[13] This relation is expressed as follows,

$$\mathbf{K_{oc} = K_d / f_{oc}} \qquad \mathbf{(1.2)}$$

where f_{oc} is the fractional mass of organic carbon in the sediment; K_d is the equilibrium distribution coefficient; and K_{oc} is the partition coefficient related to the organic carbon content of the solid. The magnitude of the coefficient, K_{oc}, is an indicator of the tendency of an organic compound to be distributed in the aqueous or the solid phases. According to this model, it is assumed that only the organic matter in the soil or sediment (expressed in terms of carbon content) is responsible for the sorption.

Because of the relatively high affinity of organic matter for hydrophobic organic compounds, other equations have been derived to relate the partition coefficient to the hydrophobicity of the organic compounds: [10,13]

$$\log K_{oc} = a \log K_{ow} + b \quad (1.3)$$

where K_{ow} is the octanol - water partition coefficient, (i.e., C_o / C_{aq}, where C_o and C_{aq} are the concentration of analyte in octanol and water, respectively) and, *a* and *b* are empirical constants. The octanol water coefficient, K_{ow}, is considered to be a measure of the hydrophobicity of the organic compound. It characterizes the partitioning of the hydrophobic compound between two immiscible liquids at the equilibrium stage. A relatively small value of K_{ow} indicates the preference of the organic compound for the aqueous phase, whereas a relatively large value of K_{ow} is indicative of its preference for the organic phase.

Another partition constant, K_{om} (similar to K_{oc}), is the partition coefficient expressed in terms of the total organic matter content of the solid. Logarithmic relations between K_{ow} and K_{om} have also been established from experimental data and have the form:

$$\log K_{om} = a \log K_{ow} + b \quad (1.4)$$

These empirical relationships enhance our ability to predict the equilibrium sorption distribution of organic pollutants in contact with natural solids when the organic content of the solid is known.

1.3.2 Interactions with Mineral Fraction

Although in several studies the validity of the above described empirical relations has been confirmed using sediments and soils that have significant carbon content and

which are from different geological origin, limitations have been identified when trying to describe the distribution of the organic compound on solids with *low* carbon content.[6,8,9,17] It has been reported that the K_{oc}-K_{ow} or K_{om}- K_{ow} relationships do not include the potential contribution of the mineral fraction to the sorption of hydrophobic organic compounds. Murphy et al.[14] studied the effect of clay and organic matter on the sorption of PAH by soils with a wide range of organic matter contents. The magnitude of the sorption constant K_d obtained experimentally was in good agreement with the predicted K_{oc} value when the percentage of organic carbon was significantly larger than the mineral content. The value of K_{oc} was underestimated when the ratio of organic carbon to mineral content (montmorillonite) was < 0.1.

The sorption of hydrophobic organic compounds has not only been related to the total quantity of organic carbon present in the natural material but also to the properties and composition of the organic carbon. It has been demonstrated that stronger sorption of hydrophobic organic compounds occurs with certain fractions of organic carbon more than with others.[14] PAH sorption has also been demonstrated to correlate more strongly with the humic acid form of organic carbon than with the total organic carbon.[15] Furthermore, it has been reported that humic acids sorb more pyrene than fulvic acids.[16]

Among the natural earth sorbents, in which organic matter content is low (< 1%) or the ratio of organic carbon to mineral content favors the mineral fraction, the sorption of organic species is dominated by the mineral content. Sorption of hydrophobic organic compounds from the aqueous phase to mineral surfaces is considered to be a non-specific interaction and might occur when one sorbate molecule displaces more than one water molecule on the solid.[6,11] The factors that influence sorption of organic compounds by the mineral surfaces of natural earth sorbents, are still debated. For example, there is still

disagreement on whether it is the *type* of mineral surface or the *nature* of the mineral-organic carbon interaction that is the most important factor in the sorption of non-ionic hydrophobic organic compounds.[6,7,17]

Even though numerous physical, chemical and biological interactions can obscure the role of any single component, it is generally accepted that among the constituents of the mineral fraction, clay minerals are the most important materials influencing the sorption of organic molecules. It has been observed that the sorption of organic compounds increased with increasing clay content in soil or sediments.[15,18,19]

Ghosh and Keitnath[19] have demonstrated the impact that different mixtures of clay materials have on the sorption of PAHs in artificially constructed soils. These authors reported that soils containing montmorillonite and vermiculite minerals had a greater capacity to sorb naphthalene compared to soils containing illite and kaolinite minerals. Murphy et al.[14] observed that humic acid rich soils containing hematite sorbed greater amounts of anthracene, dibenzothiophene, and carbazole compared to those containing kaolinite. The authors attribute these differences in sorption to conformational changes in the humic materials that are induced by the clays' hydroxyl functional groups. The hydroxyl groups are more exposed in hematite, having more binding sites to interact with the humic acid and thus allowing the humic substance to adopt a more open structure on the surface, yielding a larger hydrophobic area than kaolinite. [14]

Changes in physical properties of the sorbent such as ionic strength, pH and cation exchange capacity can affect the surface of the solid and, consequently, its ability to sorb material. However, it has been demonstrated that changes in these properties do not affect significantly the sorption of hydrophobic organic compounds onto mineral soils or sediments.[8] For example, Eisenreich and co-workers[3] showed that no correlations existed

between the sorption equilibrium distribution coefficients, K_d, and the ionic strength or the pH of the solution of a series of chlorobenzene and alkyl benzene sorbates in contact with well-characterized mineral oxides such as Al_2O_3 and FeO_3.

1.4 Kinetics of Sorption

Sorption kinetics describes the rate of transport and distribution of the sorbate between sorbed and free states. Many natural transformation processes and their rates of transport are sensitive to the distribution of the sorbate between the sorbed and free states. The study of sorption kinetics can provide information about the availability of compounds for microorganisms, the potential occurrences of chemical reactions, and the fate of organic compounds.

1.4.1 Models of sorption kinetics

Mathematical expressions used to model the kinetics of sorption are designed to provide an accurate mechanistic picture of the sorption process at the molecular level. Pignatello[7] has reviewed several sorption kinetic models. Two main groups have been identified: non-diffusion kinetic and diffusion kinetic models. Non-diffusion models treat sorption as a surface process. Information about particle geometry is not necessary, and it does not account for diffusion phenomena. Diffusion models, on the other hand, consider sorption as a diffusion-limited process at some stage during the establishment of equilibrium.[7]

The one-box and two-site models are examples of non-diffusion kinetic models; and a representative example for diffusion kinetic models is the radial diffusive penetration model.

Briefly, the one-box describes the sorption kinetics using one rate coefficient (k). This implies that all the sites in the solid are equally accessible. Modifications to the initial model have been introduced,[21] and aspects such as fraction of surface area covered, concentration of the sorbate and free energies of activation were included to evaluate the rate coefficients of the sorption process.

In the two-site model, two classes of sorption sites are distinguished in the sorbent: easily accessible sites and difficultly accessible sites,

$$Cs \underset{k_{-1}}{\overset{k_1}{\rightleftharpoons}} S_1 \underset{k_{-2}}{\overset{k_2}{\rightleftharpoons}} S_2 \qquad \textbf{(1.5)}$$

where C_S, S_1, and S_2 represent the dissolved species in solution, labile sorbed, and non-labile sorbed, respectively. This model requires three independent fitting parameters: k_1, the exchange rate from the solution to the first (accessible sites) box; k_2, the exchange rate from the first box to the second box (difficult accessible sites); and x_1, the fraction of total sorption capacity that represents the number of sorption sites in the first box.[22]

The radial diffusive penetration model modified by a retardation factor considers micro-scale partitioning of the sorbate between intra-aggregate pore fluids and the solids making up the aggregate grains. This model assumes that the sediment and soil particles are aggregates of fine mineral grains and organic matter, and that the organic compounds diffuse through the pore fluids between the interstitial regions of the aggregates. Also,

the distribution of the organics is retarded by micro-scale partitioning between a mobile and an immobile state of the chemical.[21]

The above-mentioned mathematical approaches have been used to evaluate sorption kinetic of hydrophobic organic substances in contact with sediments or soils.[21-23] Wu and Gschwend[21] evaluated the previously described models, to study the kinetics of sorption of a series of chlorobenzenes on soils or sediments using a batch technique. The one-box model was inconsistent with their data. On the other hand, the two-site model fitted the data better, although it was proposed that the reason for this better fit could be due to the greater number of fitting parameters, i.e., k_1, k_2, and x_1. According to Wu and Gschwend,[21] a disadvantage of the two-site model is the difficulty to obtain experimentally the three parameters, k_1, k_2, and x_1, and to relate them to known properties of the material. With the radial diffusive penetration model, the sorption of chlorobenzenes on sediments was explained better by adjusting the effective intraparticle diffusivity parameter (D'_{eff}):

$$D'_{eff} = \frac{D_m P_s}{(1-P_s)\rho_s K_p} \qquad \textbf{(1.6)}$$

where D'_{eff} is given in $cm^2\ s^{-1}$, K_p is the partition coefficient, D_m is pore fluid diffusivity of the sorbate ($cm^2 s^{-1}$), P_s is the porosity of the sorbent (cm^3 of fluid-filled pore space/ cm^3 total (or bulk) pore space) and ρ_s is the specific gravity of the sorbent ($g\ cm^{-3}$). Even though the authors assumed the geometry of the pore to be equaled to a constant value of 1, a satisfactory description of sorption of chlorobenzenes on sediments was achieved.[21] A major disadvantage associated with the radial diffusive penetration model is that it

requires detailed information on the physical structure of the sorbent, as well as a priori knowledge of the mechanism of sorption or the commitment to a particular one.[24]

Presently, none the available models can describe accurately the sorption kinetics of real environmental biphasic systems (i.e., dissolved and solid phase), and therefore, combination of two or more models is likely necessary to fully explain the sorption kinetics of organic compounds on natural solids.

The problems mentioned by Wu and Gschwend,[21] and noted by Pignatello,[22] and Brusseau and co-workers[23] have been treated by Gamble and co-workers.[4,25-29] A different strategy has been proposed to address the kinetic studies of organic compounds in geosorbents. This strategy has two parts: experimental and conceptual. The experimental part includes the use of online HPLC microextraction method, which avoids the problem mentioned by Pignatello of too many parameters being estimated by empirical curve fitting of the same measurements. The conceptual part uses fundamental concepts of classical chemistry (i.e., chemical units - mol/L, chemical stoichiometry, law of mass action for equilibria), labile sorption capacity of the solids, and equilibrium constants of sorption. These concepts are introduced as essential elements of sorption studies. This strategy has been applied in this work for the study of the sorption kinetics of naphthalene onto sediments.

1.4.2 A Description of Sorption Kinetics

Experimentally it has been observed that sorptive uptake of organic compounds by natural particles occurs as a bimodal process, i.e., an initial rapid uptake followed by a slower sorption process. Differentiation between these two stages of the sorption process is arbitrary and has been operationally defined.[8,13,30] Similar to sorption, desorption of

organic compounds from natural solids has also been found to proceed in two stages.[9,31,32] Thus, two fractions of sorbed compound can then be distinguished: a loosely bound, or, 'labile sorbed' fraction that easily desorbs; and a remaining amount that does not extract quickly, and which remains tightly sorbed in the solid. This second fraction contributes to the formation of an apparent 'bound residue'. It is important not to discount this second fraction because it can later diffuse back into the environment or leach out into the aquatic system and become bioavailable.[13]

The overall process can be expressed schematically as described in the two-site model:[22]

$$Cs \underset{k_{-1}}{\overset{k_{B1}}{\rightleftharpoons}} S_1 \underset{k_{-2}}{\overset{k_2}{\rightleftharpoons}} S_2 \qquad \textbf{(1.7)}$$

where C_S, S_1, and S_2 represent the dissolved species in solution, labile sorbed, and bound residue (or non-labile sorbed), respectively. Kinetic rate coefficients for sorption, ($\mathbf{k_{B1}}$, in L mol^{-1} day^{-1}), desorption, ($\mathbf{k_2}$, in day^{-1}), intraparticle sorption ($\mathbf{k_{-1}}$, in day^{-1}) and intraparticle release ($\mathbf{k_{-2}}$, in day^{-1}).[4]

The amount of labile sorbed fraction depends of the labile sorption capacity of the sediment. Labile sorption capacity is defined as the number of moles of sorbate that is reversibly sorbed by a gram of sorbent (i.e., soil or sediment), measured at the saturation limit. It is given by the following material balance equation: [4,25]

$$\theta_t = \theta_0 + \theta_1 \qquad \textbf{(1.8)}$$

where θ_t is the labile surface sorption capacity in moles per gram of solid, and θ_0 and θ_1 (mol/g) are the unoccupied and occupied active sites of the solid.

The rate of removal of the sorbate from solution (R_f) is described by a second order kinetic expression:

$$R_f = (dM_1/dt)_f = -k_{B1}\theta_0 M_1 \quad \textbf{(1.9)}$$

where M_1 is the solution concentration (mol/L). This process becomes pseudo-first order, when one of two sets of conditions is fulfilled. The first one is when the solution concentration is relatively large and the ratio of solid to solution is sufficiently small, then M_1 can be considered as constant, while θ_0 decreases. The sorbate removal from solution then becomes pseudo-first order with the apparent rate coefficient as described in Equation 1.10.

$$k_1 = k_{B1}M_1 \quad \textbf{(1.10)}$$

The second one is when the solution concentration is low, and the ratio of solid to solution is sufficiently high, so θ_1 is small, $\theta_1 << \theta_0$. Then θ_0 remains approximately constant, while M_1 decreases significantly. A different pseudo-first order rate constant is obtained as shown in Equation 1.11

$$k'_1 = k_{B1}\theta_0 \quad \textbf{(1.11)}$$

Desorption is described by a first order kinetic expression as given in Equation 1.12.

$$R_r = (dM_1/dt)_r = k_{-1}\theta_1 \quad \textbf{(1.12)}$$

where R_r is the rate of removal of the sorbate from the sorbent. The net rate of change of solution concentration can then be described by

$$\Delta R = R_f + R_r = -k_{B1}\theta_0 M_{1+} k_{-1}\theta_1 \quad \textbf{(1.13)}$$

When equilibrium has been established, Equation 1.13 reduces to the relationship

$$K_1 = k_{B1} / k_{-1} = \theta_1 / (\theta_0 M_1) \quad \textbf{(1.14)}$$

in which K_1 is the weighted average equilibrium function. This function is expressed as an average function since sediment particles contain regions that may differ in the types, amounts, and distributions of organic and mineral materials, even at the particle scale. This function accounts for sorption site heterogeneity.[21,33,34]

1.4.3 Current Methods to Follow Kinetics of Sorption

One of the most important aspects of kinetic studies is the selection of adequate methodology to measure kinetic parameters. Misinterpretation of data and false reports of kinetics occur when the limitations of the methodology used are not properly considered. This section presents a brief discussion of the advantages and disadvantages

of the currently available methodologies and those traditionally used to study sorption kinetics of earth materials.

1.4.3.1 Batch Techniques

The majority of investigations reported in literature have employed batch techniques to study sorption kinetic processes on soil/sediment constituents. Essentially, batch techniques involve placing the sorbent and the sorptive material in a mixing vessel. The resultant suspension is stirred or agitated. After a known contact time, the samples are decanted or filtered following centrifugation, and the supernatant solution is analyzed. This method primarily allows the measurement of transport and diffusion-controlled processes, thus the consequent determination of the apparent rate laws and rate coefficients.[35]

The limitations potentially encountered upon application of this methodology can be summarized as follows: the use of centrifugation as a separation method typically requires up to five minutes for adequate separation of the solid from the solution phase and many sorption processes on soil constituents are completed by this time. Yet another potential problem with batch methodology is the quality of mixing of the sorbate and sorbent materials. If mixing is inadequate, the rate of the sorption process is small and sorbate uptake is limited only to exposed sorbent material. On the other hand, the use of vigorous mixing can cause abrasion of the earth material leading to changes in the rates of reaction and in the surface chemistry of the particles.[35] Finally, the inability to remove any desorbed species poses a difficulty. The presence of desorbed material inhibits further sorbate release and can indirectly promote other types of unwanted process such as secondary precipitation reactions.[35, 36]

1.4.3.2 Flow and Stirred Flow Methods

Traditional flow methods in principle are similar to liquid-phase chromatography, i.e., it uses a column packed with the sorbent material. The sorbate is forced to flow through the column constantly by means of a peristaltic pump. Samples are then collected at various time intervals. The sorption/desorption processes are followed by monitoring concentration changes of the dissolved sorbate as a function of time. These techniques allow one to monitor sorption/desorption processes at rapid intervals (~1min), and are generally used to simulate solute transport in soils and sediments. [35]

The kinetics of sorption requires experimental techniques that do not modify the sorbate concentration significantly, thus the test samples and samples aliquots have a similar solid to solution ratio at all times. Kinetic batch studies involve large solution to solid ratios where the concentration of the sorbate in solution and the quantity sorbed vary simultaneously. With flow methods, usually small solution to solid ratios are used (typically <1), and are maintained constant for the duration of the experiment. An inherent advantage of these methods over static ones is the increased exposure of sorbate to a greater mass of sorbent, since there is a continuous flow of sorbate through the column.

Complete mixing of the sample is required in order to have a uniform distribution of particles in the sample. In flow methods, it is commonly found that colloidal particles are not dispersed evenly in the sample and this causes differences in the time required for the analyte to travel throughout the column, which in turn causes significant mass transfer differences. Furthermore, since mixing is achieved through sample flow, there may be imperfect mixing, and thus the concentrations of the analyte in the flow chamber and

effluent may not be equal. Lack of adequate mixing in a continuous flow method also results in pronounced sorbate diffusion and the determination of inadequate apparent rate parameters.

The stirred-flow technique is an improvement over the continuous flow method. The method has a better mixing of the slurry so that the analyte concentration in the chamber and effluent is same, and any transport phenomena is significantly minimized. With the stirred-flow technique the removal of the desorbed analyte is possible at each stage of the sorption process.[35]

1.4.3.3 Purge Techniques

One example of a purge technique is the gas stripping method. Consistent with this method, the analyte is removed from the aqueous phase by continuous gas stripping and then collected onto a sorbent material. The analyte is extracted subsequently using a combination of various organic solvents. The extract is then analyzed using typically UV spectroscopy or electron capture gas chromatography. It has been reported that the gas stripping method can be improved by omitting the trapping device.[24] Utilization of this technique is limited to volatile compounds and to systems in which the gas-phase concentration is of sufficient magnitude to be detected. The viable range of the gas stripping method could be extended to compounds with low Henry's Law constants using trapping devices but this is generally inconvenient because the data acquisition becomes time demanding and also because of significant data scattering in replicate analysis.[22]

1.5 The Present Research

Predictive engineering calculations require quantitative molecular level mechanisms that link the effects to causes that drive the sorption processes. Complexity of computer programs grows exponentially with the increased complexity of the overall chemical nature of the system under investigation. In addition, the variability of geosorbents also contributes to an incomplete understanding of their mechanisms of interaction.[27] The use of correlations among kinetic and equilibrium constants and the physical - chemical information of the hydrophobic organic compounds and the types and amounts of chemical materials of the soils, can provide a reasonable picture of the whole system without the need to gather specific information about each possible case (geosorbent - hydrophobic organic compound). The determination of rate coefficients representative of each category of soil - sediment material and hydrophobic organic compounds, is the first step towards the construction of a database that can be used to improve computational predictive calculations, making them more reliable and less site specific.[25-27] Gamble and collaborators have begun the compilation of such information. They investigated the interactions of pesticides - soils using an online high-performance liquid chromatography (HPLC) microextraction method developed for such systems.[4,25-28]

Gamble's online HPLC microextraction method differs from the traditional methodologies that have been focused on measuring the analyte in only one state (free or sorbed), and the concentration of the analyte in the remaining state to be deduced,[8,9] by distinguishing among dissolved, labile sorbed, and unrecoverable sorbate (i.e., bound residue), in aqueous slurries of sorbent.[28]

A few laboratories have used this methodology and it has been shown to be a practical tool to study the kinetics of sorption. Molecular level physical-chemical parameters such as labile surface sorption capacities, sorption - desorption kinetic rate coefficients, and law of mass action equilibrium functions have been obtained for pesticide - soil cases.[4,25-28]

The aim of the present study is to adapt and test an online HPLC microextraction and offline separation methods for the investigation of the chemical interaction between PAHs and marine sediments. The applicability of these methodologies to determine quantitatively the sorbate distribution in a solid-aqueous system and, to follow the kinetic of sorption will also be investigated.

Chapter Two presents the detailed development of this methodology using naphthalene as a test probe for volatile analytes. In *Chapter Three*, results of the application of the online HPLC microextraction and offline separation for the investigation of the kinetic of mass transfer of naphthalene from aqueous solution to the labile sorbed, bound residue, and possible atmospheric vapor states are presented.

CHAPTER TWO

2 DEVELOPMENT OF THE HPLC MICROSEPARATION TECHNIQUES

2.1 Introduction

A quantitative description of the different fractions in which pollutants are distributed over time is essential for increasing our understanding of the persistence, leaching risks and bound residue interference of these pollutants in soil - sediment natural aquatic systems. The complete analysis of the distribution of the analyte in the system would require chemical analyses of the analyte in all free and sorbed species (or states). Monitoring of these species throughout a kinetic experiment has not usually been possible. The products in free state are often the only species measured, and thus important information about the sorption kinetics is missed. An experimental methodology proposed by Gamble and collaborators[4,28,37-39] allows measurement of these species.

The high-performance liquid chromatography (HPLC) analytical method developed by Gamble and co-workers for pesticide - soil analysis,[4,28,37-39] has been adapted to meet the requirements of the present study, i.e., a kinetic speciation study of PAHs uptake in heterogeneous systems. This modified technique is unique among similar published methods in that it can quantitatively determine the sorbate distribution among the dissolved, labile surface sorbed, and bound residue as well as monitor their

kinetics of mass transfer among the three states (dissolved, labile sorbed, and bound residue).

This chapter provides a complete description of the development of the analytical methodology proposed to study the kinetics of sorption of PAHs in marine sediments. Details of the experimental methodology are presented and followed by the results of its evaluation. Raw data treatment is briefly discussed in the context of kinetic curves construction.

2.2 Experimental

2.2.1 Materials and Reagents

Naphthalene [Reagent Grade; Fisher Inc.] was chosen as the representative PAH sorbate molecule for this work and was used as received. Reasons for choosing naphthalene are given in *Chapter Three* of this work. Stock solutions of naphthalene 1.000 x 10^3 mg/L were prepared in acetonitrile [HPLC Grade; Caledon] and working solutions were prepared by subsequent dilution of appropriate aliquots of stock solution in water. All water used throughout this work was HPLC grade [Caledon]. All solutions were stored at 4 °C in amber glass bottles and sealed with Mininert® syringe valves 24-400 screw caps [Dynatech, VWR Canlab] to avoid decomposition and evaporation. The mole fraction of organic solvent present in solution for all sorption experiments was always less than 10^{-2}.

A sample of sand [Standard Ottawa, Silicon dioxide, Anachemia] was used as preliminary sorbent to evaluate the performance of the HPLC system, and the conditions of the experimental procedures.

Slurries were prepared and kept in 30 mL amber glass vials capped with Mininert® syringe valves during the sorption kinetic experiments. The vials were set in 50 mL jacketed beakers [Kontes] at 25.0 ± 0.2 °C and with constant stirring. A schematic description of the system is given in Figure 2.1.

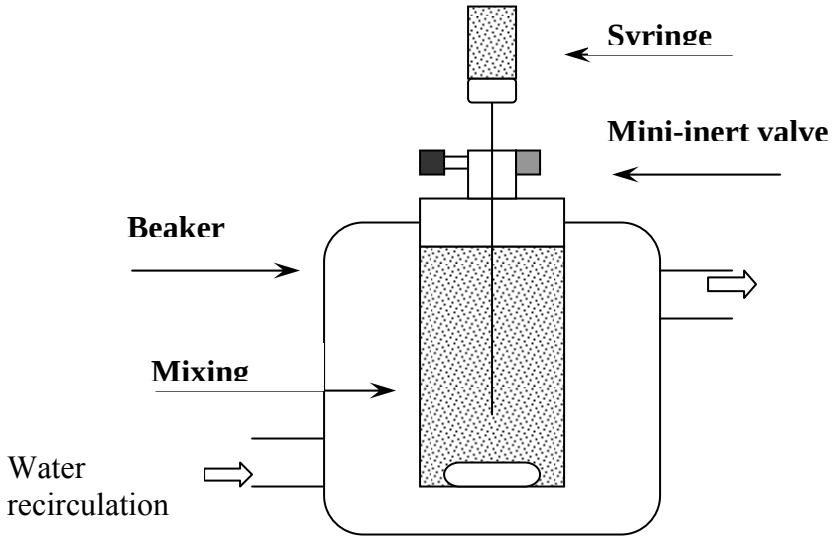

Figure 2.1. Schematic representation of mixing vessel

2.2.2 High-Performance Liquid Chromatography Systems

2.2.2.1 Offline Separation Analyses

Analyses of the sediment slurries using an offline separation method were carried out using an HP Series 1100 HPLC system [Hewlett-Packard, Agilent Technologies]. The HPLC system consisted of the following components placed in tandem: HP G1313A autosampler; an HP G1312A binary pump; an HP G1316A column thermostat set at 25 °C; an HP G1322A degasser unit; and an HP G1315A diode array UV-Vis detector. A reversed-phase analytical column Eclipse XD8C_8, dimethyl-n-octylsilane, 7.6% carbon load, [Agilent Technologies], of 4.6 mm internal diameter, 150 mm length, and 5 μm particle diameter, was used for the chromatographic determinations, and a reversed-phase Eclipse XD8C_8 guard column [Agilent Technologies], having 4.6 mm internal diameter, 12.5 mm length, and 80 A pore size preceded the main column. Figure 2.2 shows a block diagram of a conventional HPLC system.

2.2.2.2 Online Microfiltration Analyses

A conventional HPLC system [Varian, Canada] was adapted for online microfiltration of solids.[4,28,37-39] The instrumental assembly consisted of a ProStar 230 solvent delivery system, a ProStar 330 photo-diode array detector (PDA) and an injection system all in series. The injection system was modified to carry out the microextraction of the sorbate online and to carry out the subsequent removal of the sorbent particles by forcing a solvent to flow at countercurrent (i.e., backflush) through the extraction cell. This injection system is comprised of two valves: 1) an injection valve [Rheodyne 7125, Alltech] equipped with a 20 μL sample loop and, a column inlet microfilter (i.e., the

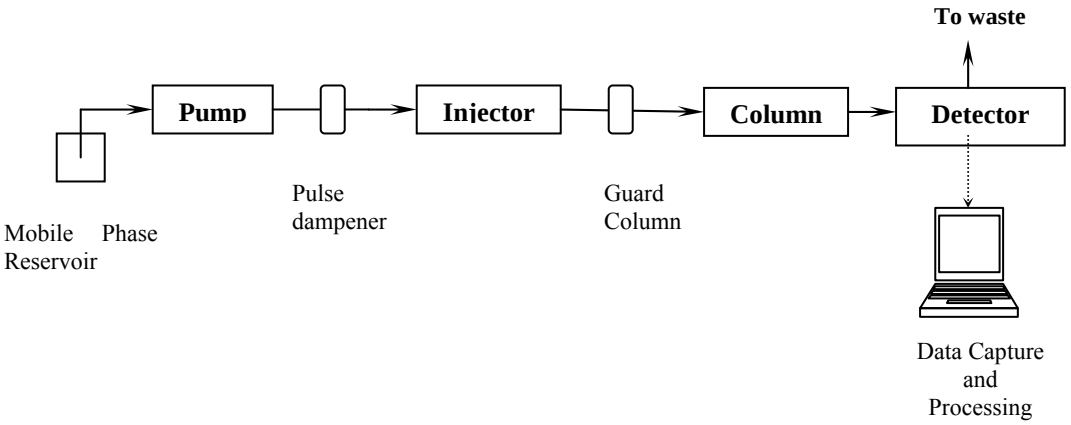

Figure 2.2. Block diagram of a conventional HPLC system

extraction cell) set with a 0.5 μm stainless steel frit [Rheodyne 7335, Alltech] and; 2) a two-positions six-port switching valve [Rheodyne 7000, Alltech]. An HPLC ternary pump [Varian 9012] connected to one of the ports of the injection valve was used to backflush the microfilter. A schematic description of the injection system is presented in Figure 2.3.

A reversed-phase analytical column LC-18, octadecylsilane, 11% carbon load, [PAH-Supelcosil, Supelco], of 4.6 mm internal diameter, 150 mm length, and 5 μm particle diameter was used for the chromatographic separations. It was preceded by a guard column LC-18 pellicular cartridge [Supelguard, Supelco] of 2 cm length, and 4.6 mm internal diameter.

2.3 Results and Discussion

2.3.1 Instrumental Conditions

Table 2.1 shows the liquid chromatography instrumental conditions used to follow the kinetics of sorption of naphthalene in marine sediments.

For the online microfiltration system, cleaning of the microfilters was performed after each injection of slurries by forcing the mobile phase to flow through the microfilter in the reverse direction (or countercurrent) of sample injection, thus removing the particulate matter out of the microfilter cartridge. This process is henceforth referred to as backflushing the microfilter.

Figure 2.3 illustrates the sequential operation of the injector and switching valves during a typical online microextraction HPLC experiment. Configuration A of Fig. 2.3

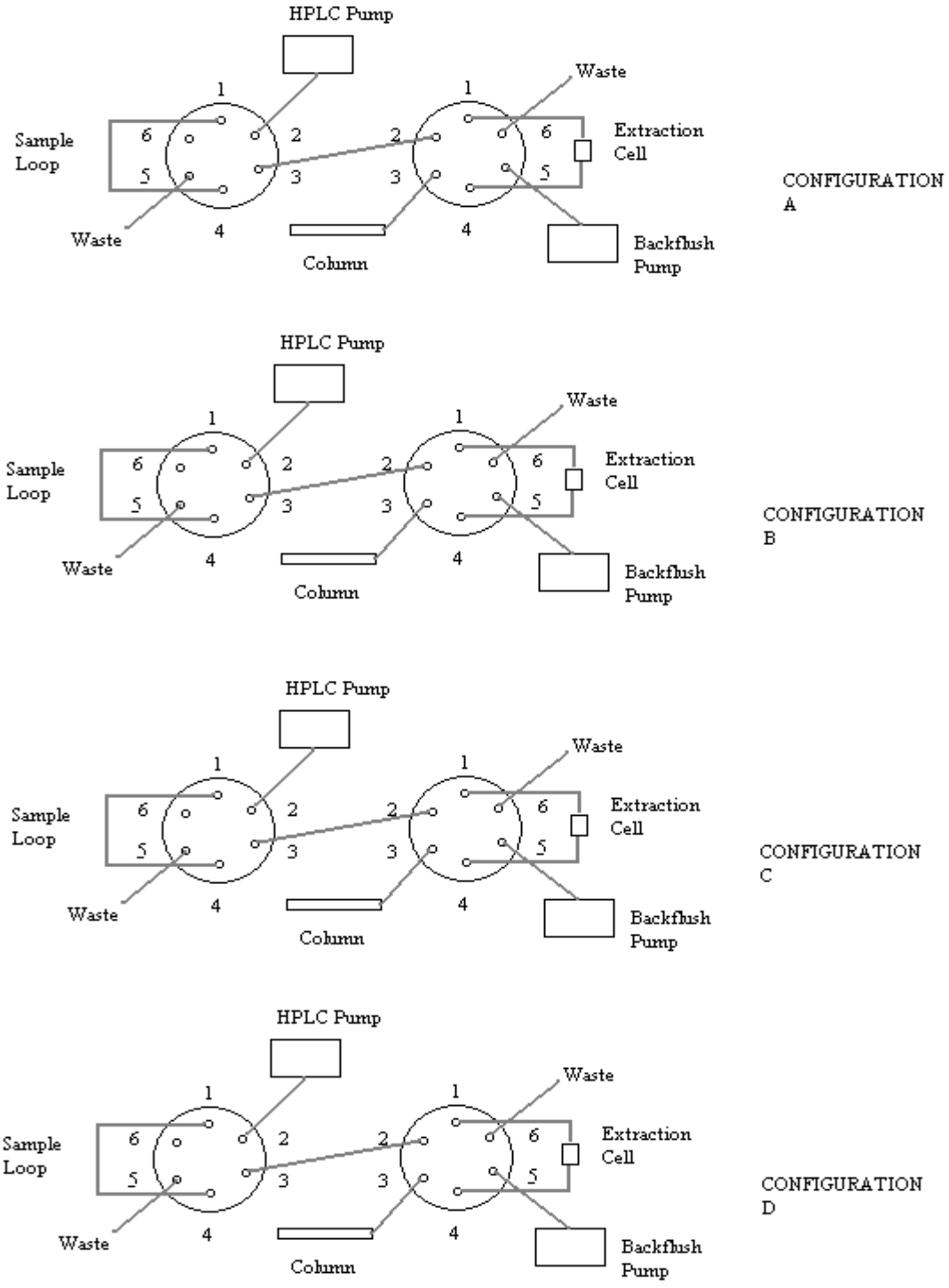

Figure 2.3. Schematic description of the injection system for online microfiltration analysis.

Table 2.1. General conditions employed for liquid chromatography

Condition	Description/Value
Mobile phase	80% Acetonitrile/ 20% Water (v/v). Isocratic elution
Flow rate	1.5 mL/min
Column temperature	25.0 °C
Injection volume	150 μL
Sample loop volume	20 μL
Diode-array detector type	Signal: 220 nm, Bandwidth 4 nm Reference: 340 nm, Bandwidth 100 nm

shows the valves' positions during the sample loading process. An excess of sample slurry is injected in the sample loop and excess material beyond the sample loop capacity is removed to waste via port No. 5 of the injector valve. The switching valve is then rotated (Configuration B) allowing the mobile phase from the HPLC pump to flow through the extraction cell. The sample slurry is then loaded in the extracted cell by positioning the injector valve in the inject position (Configuration C). The solid particles will be intercepted by the microfilter of the extraction cell, thus preventing clogging of the transfer line. The mobile phase and any dissolved and extractable species will, on the other hand, continue to migrate through the chromatographic column and the UV-Vis detector. The extraction of the slurry was allowed for 30 seconds, after which the extraction cell was isolated from the rest of the HPLC system by rotating the switching valve back to its initial position. A rinse solution (80% acetonitrile – 20 % water) was forced through the extraction cell at countercurrent via port No. 5 of the switching valve at a flow rate of 8 mL/min for 10 min using a separate HPLC pump. This rinsing step, or backflushing step, allowed an adequate cleaning of the extraction cell by removing solid particles from the cell. Visual inspection of the interior of the extraction cell confirmed the effectiveness of the cleaning process. The pressure of the HPLC system was constantly monitored to control the quality of the cleaning process.

The 30-second extraction time was determined after a series of tests whereby the extraction efficiency of the extractable naphthalene fraction (dissolved plus labile sorbed naphthalene) was measured as a function of extraction time. These tests involved essentially injecting 0.15 mL aliquots of naphthalene-spiked sand slurries (1 mg sand/mL water) in the online microfiltration HPLC system. The samples were left on the online extraction cell for different extraction times and the resultant peak area was used as

a test criterion. No further increase in the analyte peak area could be observed beyond 30 second of extraction time. The dead volume of the microextraction HPLC system was determined to be 1.6 mL. The dead volume was calculated by multiplying the retention of water (an un-retained species, r_t = 1.1 min) by the mobile phase flow rate (1.5 mL/min).

2.3.2 Evaluation of the Analytical Response

For the online microfiltration setup, evaluation of the quality of the analytical signal and the effect of introducing solid material into the HPLC system was performed. The precision of the signal, peak shape, calibration curves and limit of detection were evaluated.

2.3.2.1 Signal Precision

To verify the reproducibility of the naphthalene signal measured from the offline microfiltration system, slurry samples of sand in water were prepared. The sand was initially used to test the HPLC system prior to using actual sediment, employing comparable conditions. The sand was ground and then sifted using a 125-μm sieve. The sieved sand was subsequently used to prepare slurries with different sand/water ratios (0.5 to 1.2 mg/mL). The slurries were spiked with naphthalene to contain naphthalene concentrations in the slurry in the range of 3.9×10^{-6} to 3.9×10^{-5} M. Replicate injections of naphthalene-spiked slurries and naphthalene aqueous standard solutions were analyzed and relative standard deviations of the peak area were calculated. For slurry replicates (n = 20), the relative standard deviation calculated was in the order of 5.0%, whereas for standard solutions (n = 10), the relative standard deviation was found to be in the order of

0.50 to 1.0%. The reproducibility of the signal deteriorated to some extent from standard solution to slurry sample but such an error never exceeded 10% and thus was deemed acceptable under these experimental conditions.

2.3.2.2 Peak Shape Reproducibility

The symmetry of the chromatographic signal of the spiked slurries and the naphthalene standard solutions was evaluated. The chromatographic signals presented a Gaussian profile with asymmetry factors, determined at 10% of peak height, of 1.5 and 1.1 for slurries and standard solutions, respectively. The values obtained are in the same order of magnitude expected for analytical determinations (i.e., asymmetry factors <1.6),[40] indicating the absence of any significant distortion in the signal. Thus, it is demonstrated that the physical nature of the sample (i.e., slurry) does not compromise the quality of the analytical response of the instrument. Figure 2.4 shows a typical chromatographic signal obtained from a naphthalene-spiked slurry sample (Fig. 2.4A), a naphthalene standard solution (Fig. 2.4B), and the UV spectrum of the chromatographic peak of the naphthalene standard and the naphthalene reference spectrum from the HPLC library. Essentially naphthalene is detected at a retention time of about 1.8 min. regardless of the physical state of the sample (slurries or solution) and no peak distortion or broadening was observed for naphthalene in slurries.

2.3.2.3 Calibration Curves

A series of four naphthalene standard solutions in the range of 0.0 to 7.9 x 10^{-5} M were prepared and analyzed daily. Calibration curves were prepared using the method of least squares regression and correlation coefficients (r^2) were better than 0.995.

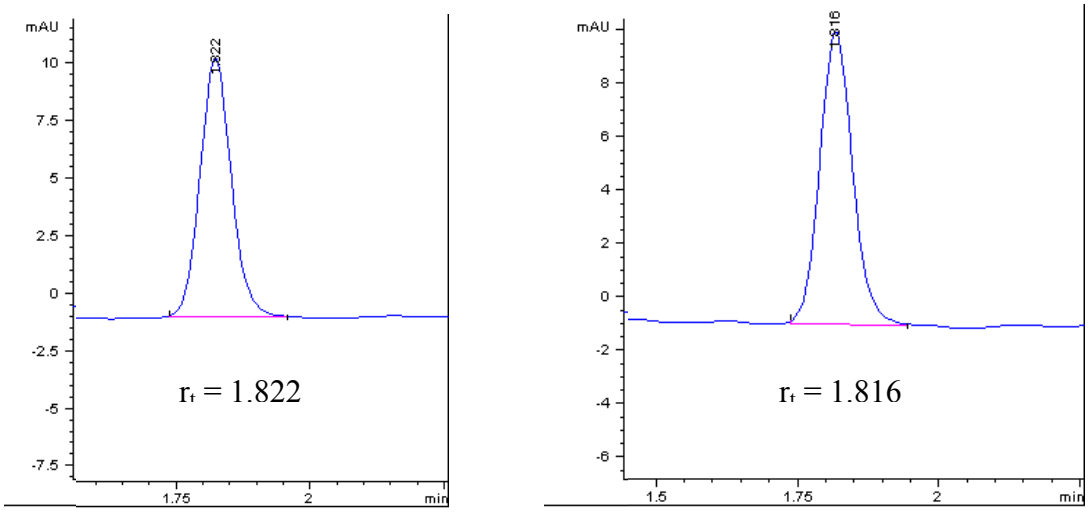

A **B**

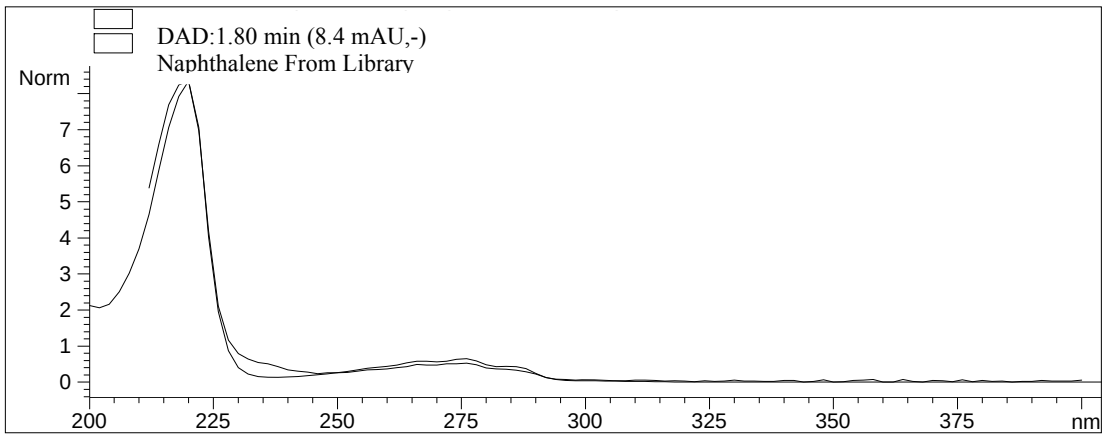

C

Figure 2.4. Typical chromatographic signals: (A) PACS-2 slurry naphthalene-spiked $1.6x10^{-6}$ M at time t = 0.5 min. (B) Naphthalene standard solution $1.6x10^{-6}$ M. (C) Spectrum of chromatographic peak (r_t=1.8 min) of the naphthalene standard as measured by the HPLC photo-diode array detector and the naphthalene spectrum from the HPLC library.

Figure 2.5 shows an example of a typical calibration curve obtained for a series of naphthalene solutions.

2.3.2.4 Limits of Detection

Blanks of the standard solutions, and of the two marine sediments PACS-2 and HISS-1, were analyzed using online HPLC microextration and offline separation methodologies to determine the limits of detection (LD) of the analytical instruments. The limit of detection was taken as three times the standard deviation of the blank over the sensitivity of the signal.[41] The limit of detection typically falls in the range of $2x10^{-8}$ to $8x10^{-8}$ M, with the average LD being $6x10^{-8}$ M. This LD is at least one order of magnitude lower than the concentration of the smallest naphthalene standard solution used.

2.3.3 Sample Preparation

Several ratios of sediment to solution were tested to find the optimum ratio of sediment to solution required for the analysis using the HPLC techniques. The criterion chosen to determine the best slurry composition was based on the effect the introduction of samples of slurry have on the pressure of the HPLC system. Best results were obtained when slurries were prepared with a ratio of mass of solid (mg) to volume of liquid (mL) of ~1. Above this ratio the pressure in the HPLC system increased significantly indicating clogging of the microfilters. The final slurry composition consisted of 25.0 ± 0.2 mg of sediment in 28.0 ± 0.5 mL of solution. Prior to beginning the kinetic

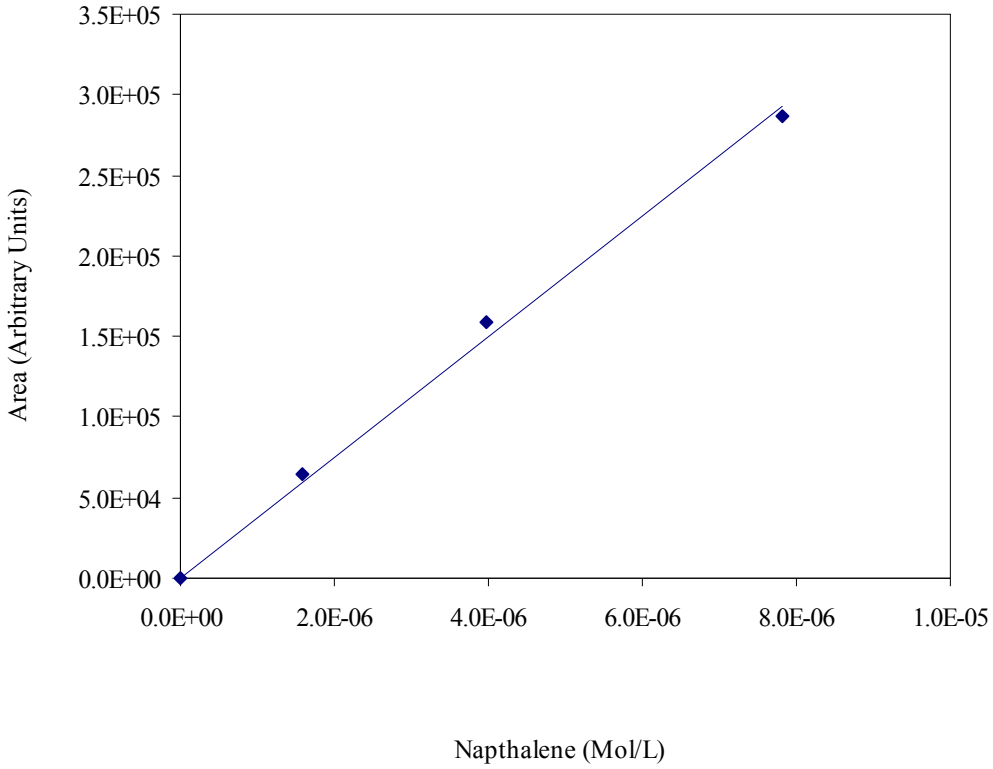

Figure 2.5. Calibration curve naphthalene standard solutions. Varian ProStar HPLC. Online microfiltration setup. Wavelength 220 nm. Best fit: Area = 3.74×10^{10} [Naphthalene]. Correlation coefficient $r^2 = 0.996$.

experiments, the sediments were conditioned by soaking pre-weighed samples of the solids in 5.0 ± 0.5 mL of water for four days at 25.0 ± 0.2 °C with continuous stirring.

This wetting period was based on reported times used to condition soils.[25,42] Wetting of sediments is important because it allows the sediment to recover its original physical and chemical characteristics.

2.3.4 Samples Control

2.3.4.1 Loss of Naphthalene

The potential for naphthalene loss simply by evaporation and loss to container inner surfaces can be significant, thus actions were taken to minimize naphthalene losses. Reaction vial caps were found to be problematic in this respect. Polypropylene caps with silicone/ PTFE septa were responsible for a 100% loss of naphthalene from samples stored for less than three days. Other types of septa and vial caps were investigated. Mininert® syringe valves, of the type described previously were found to perform the best with a total loss of naphthalene between 7 to 25% for kinetic experiments lasting from 7 to 22 days.

2.3.4.2 Naphthalene Background in Sediments

Blank slurries of PACS-2 and HISS-1 sediments were tested for naphthalene background. These slurries were prepared with the same sediment to water ratio and percentage of organic solvent used to prepare naphthalene-spiked slurries. Using the online microfiltration and offline centrifugation HPLC methodologies, analyses of slurry samples were performed and no detectable naphthalene (LD ~ 6 x 10^{-8} M) was observed

throughout the experiment. Slurries were continuously monitored over time to ascertain the absence of naphthalene in the sediments during the kinetic experiments.

2.3.5 Sorption Kinetics

The slurries were spiked with aliquots of aqueous naphthalene solutions of a known concentration. This spiking procedure is considered to be an adequate means to introduce hydrophobic organic compounds to geosorbents in aqueous media.[42] Samples of slurry (150 μL) were subsequently collected from sample vials over defined periods of time, using a 250-μL glass syringe (Hamilton 725RN, 250μL) with removable 22-gauge stainless steel needle, for the analysis of naphthalene using HPLC with UV-visible detection.

2.3.5.1 Total Extractable from Whole Slurry

With the online microfiltration HPLC arrangement, samples of whole slurry were injected directly into the system to fill a 20-μL sample loop. The sample was then loaded into the extraction cell whereby the online microfilters trapped the solid particles of the injected slurry, at which point the mobile phase served as the extracting liquid. The resulting chromatographic peak for naphthalene represented the total naphthalene present in solution and extractable from the solid particles. Each slurry injection was bracketed with standard solutions to continuously correct for any instrumental drift. After each slurry injection, the system was backflushed with rinse solution to remove the solids from the online microfilters. This cleaning routine prevented excessive pressures in the instrument, and consequently changes in analytical response.

Naphthalene loss via sorption on inner walls of the HPLC tubing or on online microfilters was evaluated by injecting in the online HPLC microfiltration system aliquots of freshly prepared naphthalene solution. Comparing results with the expected value, losses were found to be 1.5 ± 0.5 % (n = 25). These results are within the experimental error and no corrections for this effect was then required.

2.3.5.2 Total Dissolved Naphthalene

Measurements of naphthalene concentration dissolved in solution were obtained by HPLC analysis of the liquid phase of the whole slurry. Separation of the solid and liquid phases of slurry samples was performed mechanically. Two separation procedures were evaluated, filtration and centrifugation. Contact times for kinetic measurements were determined by recording the time at which the separation of the samples was carried out. These offline measurements were used to construct the naphthalene dissolved kinetic curve. Naphthalene standard solutions were subject to the same treatment, and in this way, the measurements of naphthalene concentration in solution were corrected for losses during handling of the samples.

2.3.5.2.1 Offline Microfiltration

Several filter membranes were tested using naphthalene-spiked slurries in the concentration range of interest (i.e., 1.6×10^{-6} M to 7.8×10^{-6} M). Prior to their use, filtration membranes were cleaned using mixtures of acetonitrile water (80% acetonitrile/ 20% water) and left to air dry. Slurry samples were filtered and the filtrate was analyzed using HPLC. Figure 2.6 shows a graphic representation of the percentage of naphthalene losses after the filtration process using various membranes filters and the error associate with this procedure. A description of the membranes used can be found in Appendix 1.

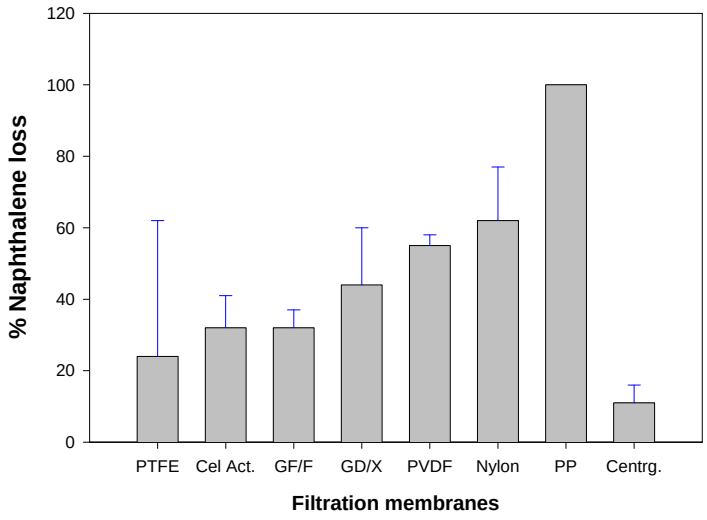

Figure 2.6. Naphthalene loss by sorption onto filtration membranes.

Loss of naphthalene due to sorption onto filtration membranes were determined to be 23 ± 4% in PTFE membranes (the smallest sorption loss) to 100% in the case of polypropylene membranes (the largest sorption loss).

2.3.5.2.2 Centrifugation

Centrifugation was used as an alternative phase separation procedure. The time required for separation of the solid and liquid phases was evaluated. Five minutes at 3200 rpm were required to achieve separation of the two phases. Qualitative evaluation of the centrifugation process was performed by inspection of the dispersion of light generated when a laser beam passed through the liquid phase. Naphthalene concentration in solution was then evaluated by HPLC and losses of naphthalene were determined. Figure 2.6 shows the percentage of naphthalene loss by centrifugation. Losses by centrifugation were determined to be 11.3 ± 3.1% (n = 20). Since centrifugation provided the smallest losses of naphthalene, it was therefore adopted as the method of choice to separate the liquid phase from the solid phase in slurry samples.

2.3.6 Data Treatment

Measurements of naphthalene concentration in standard solutions were used daily to prepare calibration curves (peak area vs. naphthalene concentration). Least squares regression fit constants were used to calculate naphthalene concentration of slurry and naphthalene solutions.

Every slurry system was prepared in triplicate, and sampling was done approximately at the same time. Every replicate result was normalized to the amount of solid used in the slurry and was used to prepare the time-dependent curves.

From the measurements of naphthalene concentration present in slurry samples using offline centrifugation and online HPLC microextraction, two time-dependent concentration curves (or kinetic curves) were obtained, *dissolved-naphthalene* (Figure 2.7A) and *extractable-naphthalene* (Figure 2.7B), respectively. Similarly naphthalene standard solutions were also analyzed over time using the two HPLC systems and under the same experimental conditions as with slurries.

The difference between the dissolved-naphthalene time-dependent concentration curves (i.e., offline centrifugation with HPLC analysis) of naphthalene standard solution and naphthalene-spiked slurries yields the *labile sorbed plus bound residue* fraction of naphthalene. The difference between the extractable-naphthalene time-dependent concentration curves (i.e., online microfiltration with HPLC analysis) of naphthalene standard solution and naphthalene spiked slurries yields the *non-labile bound or bound residue* fraction of naphthalene. Finally, the difference between the above-mentioned resultant fractions of naphthalene, i.e., the *labile sorbed plus bound residue* minus *bound residue* yields the *labile sorbed* fraction of naphthalene.

Three different time-dependent concentration curves that show the time-dependent distribution of naphthalene in the system (i.e., dissolved, labile sorbed and, bound residue naphthalene) were obtained for each set of replicate slurries (triplicates were prepared for each naphthalene concentration). The replicate kinetic curves were then averaged and curve fitted using least squares regression.

The above-described mathematical procedure allows the naphthalene concentration in the free and sorbed states to be corrected for possible loss of naphthalene by means other than sorption onto sediments, (e.g., loss of naphthalene to vapor phase). This procedure assumes that the extent of naphthalene volatilization and its transfer rate

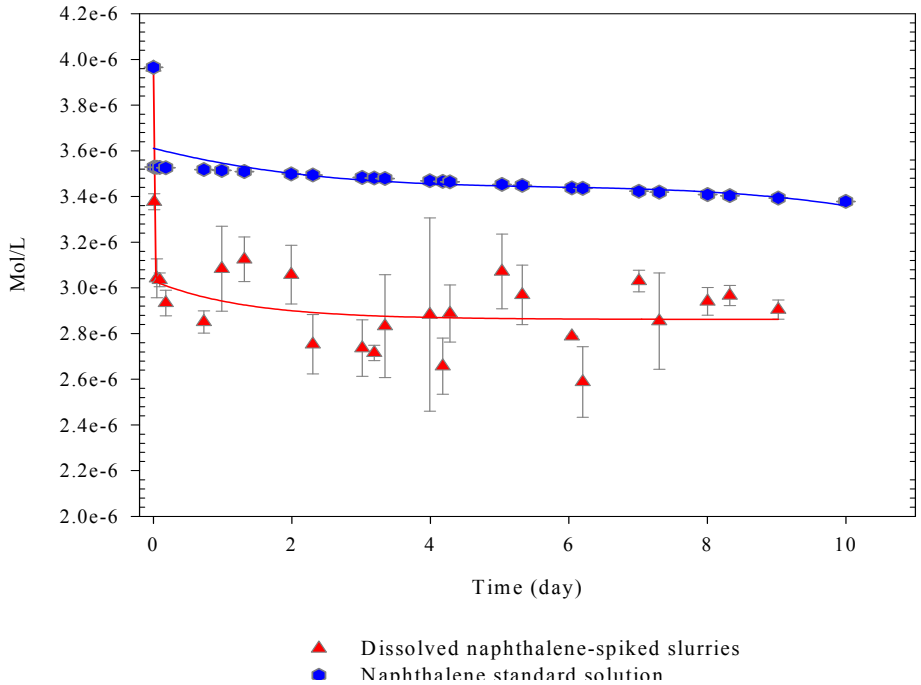

A

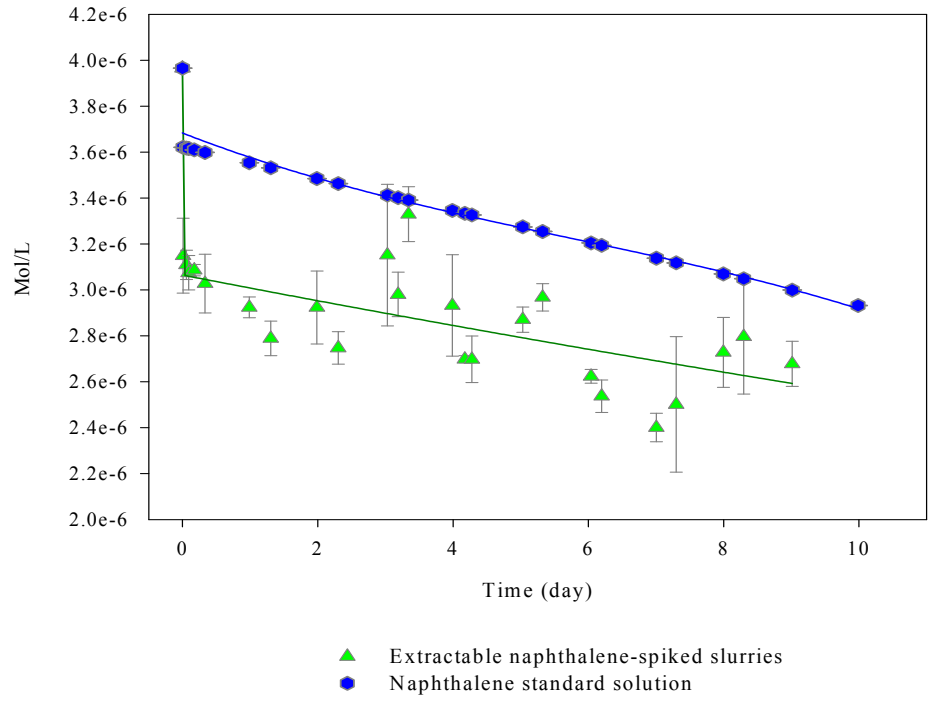

B

Figure 2.7. (A) Analysis of naphthalene standard solution and naphthalene-spiked slurries at 4.0 x10^{-6} M using HPLC offline centrifugation. **(B)** Analysis of naphthalene standard solution and naphthalene-spiked slurries at 4.0 x10^{-6} M using HPLC online microfiltration.

from solution to vapor phase (to head space of mixing vials) is the same for slurries as for the naphthalene solutions. This assumption was confirmed experimentally by analyzing naphthalene concentration in vapor phase of spiked slurries and standard solutions. The methodology used for this analysis is as follows: two sets of mixing vials were prepared. One set comprises of two replicates of naphthalene-spiked PACS-2 slurries (1.1 mg/mL sediment/solution) and the second set comprises of two replicates of naphthalene standard solution. In both cases the initial naphthalene concentration was 4.0×10^{-6} M with a final volume of 28 mL. The slurries and solutions were kept under the same experimental conditions used for the kinetic experiments (see Section 2.2.1). Aliquots of 0.15 mL were collected daily from the sample vials to create the same headspace as in the kinetic experiments (number of uptakes n=20). Triplicate analysis of naphthalene in headspace was performed using GC-FID (Varian 3800). Comparison between the mean peak area of the naphthalene chromatographic signal of the naphthalene standard solution and the naphthalene-spiked slurries showed no significant difference. In addition, the Student's t-test showed that no statistical differences existed between the naphthalene concentration in the headspace of naphthalene standard solution and that in the naphthalene-spiked slurries. Details of this experiment are presented in Appendix 2.

2.3.7 Advantages and Limitations of Microextraction

Combination of online microextraction and offline HPLC separation methodologies for sorption kinetic studies provides the opportunity of obtaining quantitative information about the free and sorbed states of the analyte. Advantages of the online microextraction HPLC technique over conventional extraction methodologies can be summarized as follows:

Extraction of sorbate from solid particles in microextraction HPLC is carried out with relatively large ratios of extractant to solid. In a typical experiment, a 20 μL aliquot would contain 18 μg of solid, and the volume of mobile phase available for eluting a labile sorbed compound is at least 50 mL per milligram of solid. This ratio is at least twenty times greater than conventional extraction methods[12] and, with the benefit of a continuous flow of fresh extracting instead of a static batch operation.

The measurement time for each point in the kinetic curves is also an important benefit of this methodology. Retention times in the online microextraction HPLC for naphthalene are in the order of 2 to 3 minutes, whereas in conventional extraction methods reflux times are in the range of 30 minutes to hours to obtain a single measurement of the sorbate bound to solid particles.

An inconvenience encountered with the online microextraction HPLC method is the amount of solids that could be introduced per injection into the system. A rapid increase in the pressure of the HPLC was observed when working with ratios of solids to liquid bigger than 25 mg/28 mL. The instability in the pressure of the system lead to poor repeatability of the chromatographic signal of sample replicates.

The online microextraction HPLC methodology has limitations with regard to the study of fast sorption kinetics (i.e., faster than 1 to 2 min). Sample loading in the HPLC is the main limiting parameters in the study of sorption kinetics. In the present investigation sorption times smaller than 2.0 minutes could not be measured since this is the minimum time required to obtain a chromatographic signal.

The range of concentration in which the sorbate can be measured is another limiting factor, and that is directly dependent on the type of detector used for the

chromatographic signals. Linear calibration curves where obtained over the concentration range used in this work.

2.4 Summary

An experimental methodology has been developed to study the sorption kinetics of PAH in sediments. The potential of this method to determine quantitatively PAH distribution between free and sorbed states in natural slurries was evaluated. An online microextraction HPLC procedure has been adapted and tested for volatile compounds. Naphthalene was used as a single chemical probe to assess the applicability of this methodology to PAH – sediment cases. A mixture of 80% acetonitrile/20% water (v/v) was used as the extractant at a flow rate 1.5 mL/min. Offline separation of the liquid and solid phases was best-achieved using centrifugation. Analyses of naphthalene in aqueous phase were performed using a conventional HPLC with UV-Vis detection. Quantification of naphthalene distribution between free and sorbed fractions in the order of 40 parts per billion (ppb or μg/L) was achieved with relative standard errors in the order of 5%. Kinetic curves with a minimum time resolution of 2 min. were obtained.

CHAPTER THREE

3 APPLICATIONS

3.1 Introduction

Naphthalene in contact with marine sediments was the system chosen to follow the kinetics of sorption of PAHs onto heterogeneous sorbent materials. Naphthalene is the smallest member of the PAH series. It is the most abundant product in coal tar distillate, and it is frequently found in PAH contaminated sites. Naphthalene is commonly used as a household fumigant against moths and has some application as a soil fumigant. Commercial production of this chemical involves the crystallization of the intermediate fraction of coal tar distillate. Naphthalene can also be produced from the heavier fractions of cracked petroleum.[43]

The interaction of naphthalene with low carbon content sediments is a limiting case among the possible combinations of PAHs and types of aquatic sediments. The high volatility of naphthalene (naphthalene vapor pressure: 36.8 Pa at 25°C),[44] and the chemical inertness of the quartz sorbents should result in an extreme case that can be used to determine a limit for the utilization of online microextraction HPLC and offline centrifugation HPLC methodologies to investigate sorption behavior of PAHs with natural solids.

The objective of the following experiments is to study the distribution of naphthalene in free and sorbed states, and to follow the kinetic behavior of naphthalene in contact with two well characterized marine sediments.

3.2 Experimental Section

3.2.1 Materials and Reagents

Naphthalene solutions were prepared as described previously in section 2.2.1. In all cases the maximum concentration of acetonitrile as a co-solvent (to facilitate the dissolution of naphthalene in water) was less than 2.5% v/v. At this concentration, acetonitrile should have little effect on the activity coefficient of the sorbate and therefore no changes in sorption conditions of naphthalene onto the sediment are expected.[45]

Two sorbent materials were studied, both marine sediments, certified reference materials for trace metals analyses from the National Research Council Canada (NRC-CNRC). HISS-1 sediment was collected from the Hibernia Shelf off the coast of Newfoundland, and PACS-2 sediment from the harbour of Esquimalt, B.C.[46] The materials were used as received except for wetting the sediment prior to a kinetic experiment. Each sediment sample was analyzed for a number of chemical properties including: pH, measured in an aqueous solution of 0.01M $CaCl_2$ in a 1:2 sediment/solution ratio;[47] electrical conductivity, measured in 1:2 sediment/solution ratio;[48] total carbon, nitrogen and sulfur contents were determined by high temperature (1450 °C) oxidation with pure oxygen (CNS-2000 analyzer Leco Inc.);[49] and hydrogen content was determined using CHN-analyzer (PSC Analytical Services). In addition, major constituents and mineralogical analyses were performed using X-ray fluorescence analysis (Philips PW2400 X-Ray spectrometer, Saint Mary's University) and X-ray powder diffraction analysis (Rigaku MiniFlex X-ray diffractometer, Dalhousie University).

3.2.2 Methodology

The HPLC instruments used for the online microextraction and offline centrifugation methods were set up as described in Table 2.1. The methodology used to follow the sorption kinetics of naphthalene in sediments was the same as described in sections 2.3.5.1 and 2.3.5.2.2. Sediments were prepared as described in section 2.3.3 "Sample Preparation" prior to their use, i.e., sediments were wetted for a minimum of four days. For each point of the kinetic curves, four types of solutions/slurries were used to monitor the sorption conditions. *Blank solutions*, containing only diluted acetonitrile (i.e., solvent) were used to correct the naphthalene standard solutions for any contribution to the naphthalene chromatographic peak (retention time, r_t, ~1.8 to 1.9 min.). The *blank sediment slurries* containing sediment and solvent were used to correct the naphthalene-spiked sediment slurries for any contribution to the naphthalene chromatographic peak. *Naphthalene standard solutions*, that contained solvent and naphthalene of known concentration, were used to correct any instrument drift and any naphthalene loss (e.g. by evaporation). The *test naphthalene-spiked sediment slurries* contained solvent, sediment, and a known initial concentration of naphthalene. Each solution/slurry was prepared in triplicate, kept at 25.0 ± 0.2°C with constant magnetic stirring.

These separate sorption kinetic experiments were initiated by spiking the slurries with dissolved aqueous naphthalene to give three different final concentrations, 1.6 (± 0.1) x 10^{-6} M, 4.0 (± 0.2) x 10^{-6} M, and 7.8 (± 0.5) x 10^{-6} M. Northcott and Jones[50] conducted a thorough review of spiking procedures typically used for the study of sorption/desorption of organic compounds with sediments or soils. These authors pointed out that the spiking procedure could have adverse and unpredictable effects on the

processes under study.[50,51] For example, the acetonitrile (the solvent carrier) used to dissolve naphthalene could change the partitioning behavior of naphthalene. According to Northcott and Jones, the spiking method (sediment/water slurry) used in this study is appropriate for the study of sorption/desorption of organic compounds with sediments.

3.3 Results and Discussion

3.3.1 Sediment Characterization

Results of the chemical and mineralogical characterization of the two marine sediments are shown in Table 3.1. Both samples present sand characteristics, with quartz as the main mineral component. PACS-2 presents higher carbon content than HISS-1 and, it has a significant content of the minerals Albite ($NaAlSi_3O_8$, feldspar), Halite (NaCl) and Clinochlore ($(Mg,Fe,Al)_6(Si,Al)_4O_{10}(OH)_8$, clay).

3.3.2 PACS-2 Sediments

3.3.2.1 Sorption Experiments

The analysis of naphthalene-spiked sediment slurries using online HPLC microextraction and offline centrifugation HPLC techniques generates two kinetic curves that represent the extractable naphthalene concentration (dissolved plus labile sorbed naphthalene) and the dissolved naphthalene concentration, respectively. Figures 3.1A to 3.1C show the extractable naphthalene kinetic curves (or time-dependent concentration curves) for naphthalene-spiked PACS-2 slurries at initial naphthalene concentrations of

Table 3.1. Chemical characterization of marine sediments.

Property	Units	PACS-2	HISS-1	Notes
pH		6.4	8.7	Measured as a 1:2 (mass:volume) ratio
Electrical Conductivity	mS/cm	21.09	4.39	Measured as a 1:2 (volume:volume) ratio
Carbon	%(w)	3.21 ± 0.15	0.39 ± 0.02	Soils results are expressed on an air dried basis
Sulfur	%(w)	1.55 ± 0.01	0.03 ± 0.01	
Nitrogen	%(w)	0.38 ± 0.03	nd	
Hydrogen *	%(w)	1.2	nd	* Estimated Quantitation Limit (EQL) 0.5. nd: not detected above standard EQL
Major constituents				
SiO_2	%	56.24	95.00	X-ray fluorescence
TiO_2	%	0.698	0.146	
Al_2O_3	%	12.09	1.28	
Fe_2O_3	%	5.69	0.36	
MnO	%	0.051	0.005	
MgO	%	2.35	0.07	
CaO	%	2.73	1.57	
Na_2O	%	4.54	0.44	
K_2O	%	1.45	0.40	
P_2O_5	%	0.222	0.027	
V	ppm	116	26	
Cr	ppm	75	14	
Zr	ppm	135	163	
Ba	ppm	1031	389	
Ni	ppm	24	<3	
Zn	ppm	352	9	
Ga	ppm	13	<5	
Sr	ppm	272	109	
Nb	ppm	9	<1	
Total	%	93.32	100.03	
Loss of ignition	%	13.47	1.60	
Mineralogical composition				
Quartz (SiO_2)	%	62.6	99.4	X-ray powder diffraction analysis
Halite (NaCl)	%	14.3	0.6	
Albite, ordered ($NaAlSi_3O_8$)	%	18.8		
Clinochlore, ferroan $(Mg,Fe,Al)_6(Si,Al)_4O_{10}(OH)_8$	%	2.8		
Calcite ($CaCO_3$)	%	1.5		

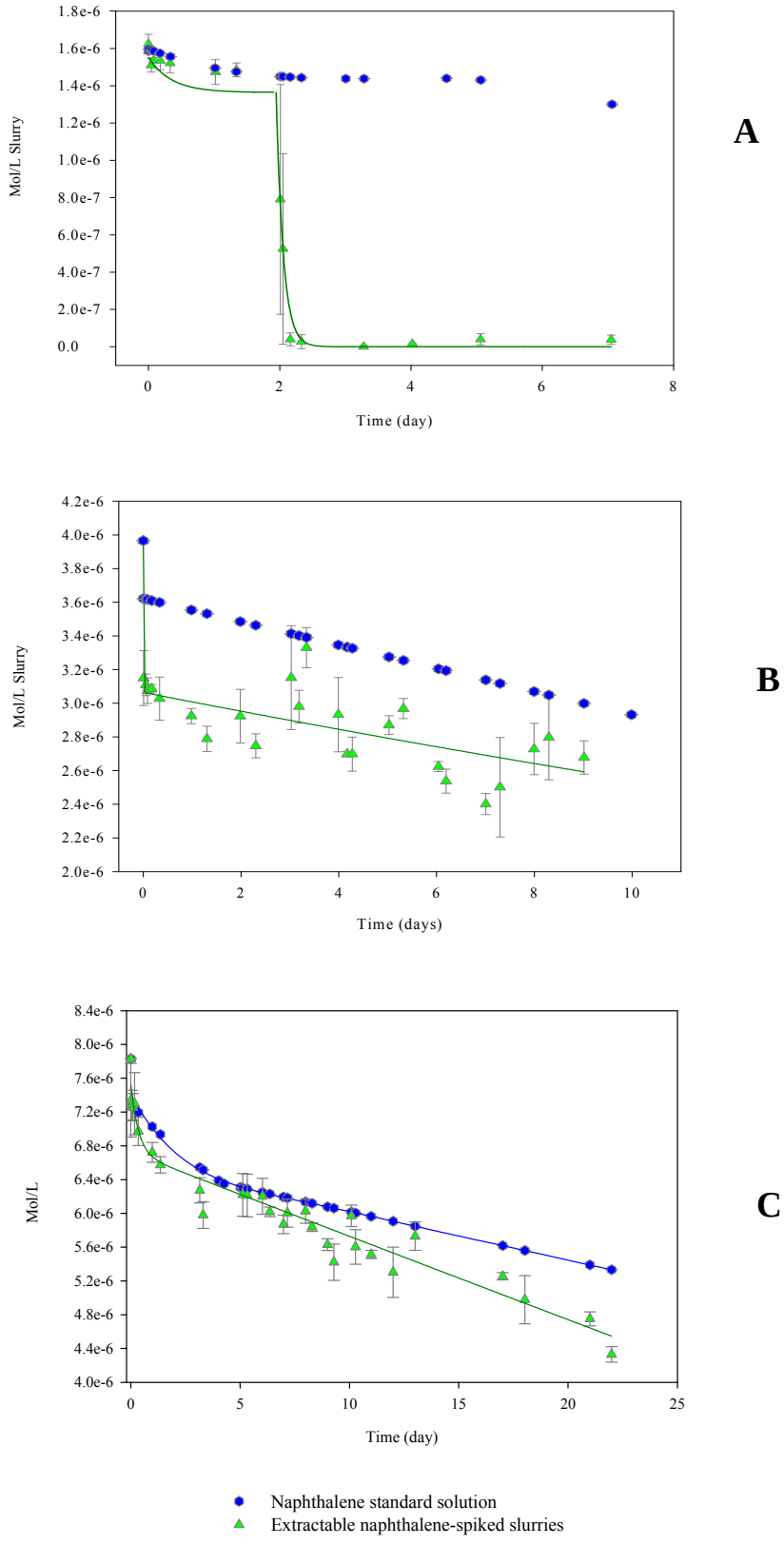

Figure 3.1. Extractable naphthalene kinetic curves from PACS-2 slurries. Initial naphthalene concentration: **(A)** 1.6×10^{-6} M, **(B)** 4.0×10^{-6} M, **(C)** 7.8×10^{-6} M at 25.0°C. Curve fitting using exponential decay.

$1.6x10^{-6}$ M, $4.0x10^{-6}$ M, and $7.8x10^{-6}$ M, respectively. Each kinetic curve is accompanied by the concentration curve of a naphthalene standard solution having the same initial concentration as the test slurries. Figures 3.2A to 3.2C show the dissolved naphthalene kinetic curves for naphthalene-spiked PACS-2 slurries together with the respective concentration curve of a naphthalene standard solution having the same initial concentration as the test slurries.

In the case of slurries spiked to an initial naphthalene concentration of $1.6x10^{-6}$ M (Figs. 3.1A and 3.2A), the two kinetic curves (i.e., extractable and dissolved naphthalene, respectively) presented three distinguishable regions. The first region corresponded to the first eight hours of contact time, in which an initial decay in the naphthalene concentration was observed. In the second region, between nine to 24 hours, a nearly constant naphthalene concentration was obtained, and in the third region, between day 1 and 2, a rapid drop in naphthalene concentration to below the detection limit (LD: $6x10^{-8}$ M) was observed. Figure 3.3 shows that the kinetic curves of two other replicate experiments of naphthalene-spiked PACS-2 slurries at $1.6x10^{-6}$ M are nearly identical to the one described in Fig. 3.1A, indicating that this experiment is highly reproducible. Contrary to the slurries, no rapid loss of naphthalene was observed in any of the replicate naphthalene standard solutions.

The rapid loss of naphthalene from solution between day 1 and 2 cannot be attributed to a chemical reaction whereby naphthalene would be a reagent because chemical reactions do not require induction time like those sometimes found for microbiological processes. The sediments were irradiated (minimum dose of 2.5 mRad = $2.5x10^{-5}$ J/kg) prior of being sealed by the manufacturer (NRC) to minimize any effect from biological activity,[46] thus the presence of microorganisms in the sediments was

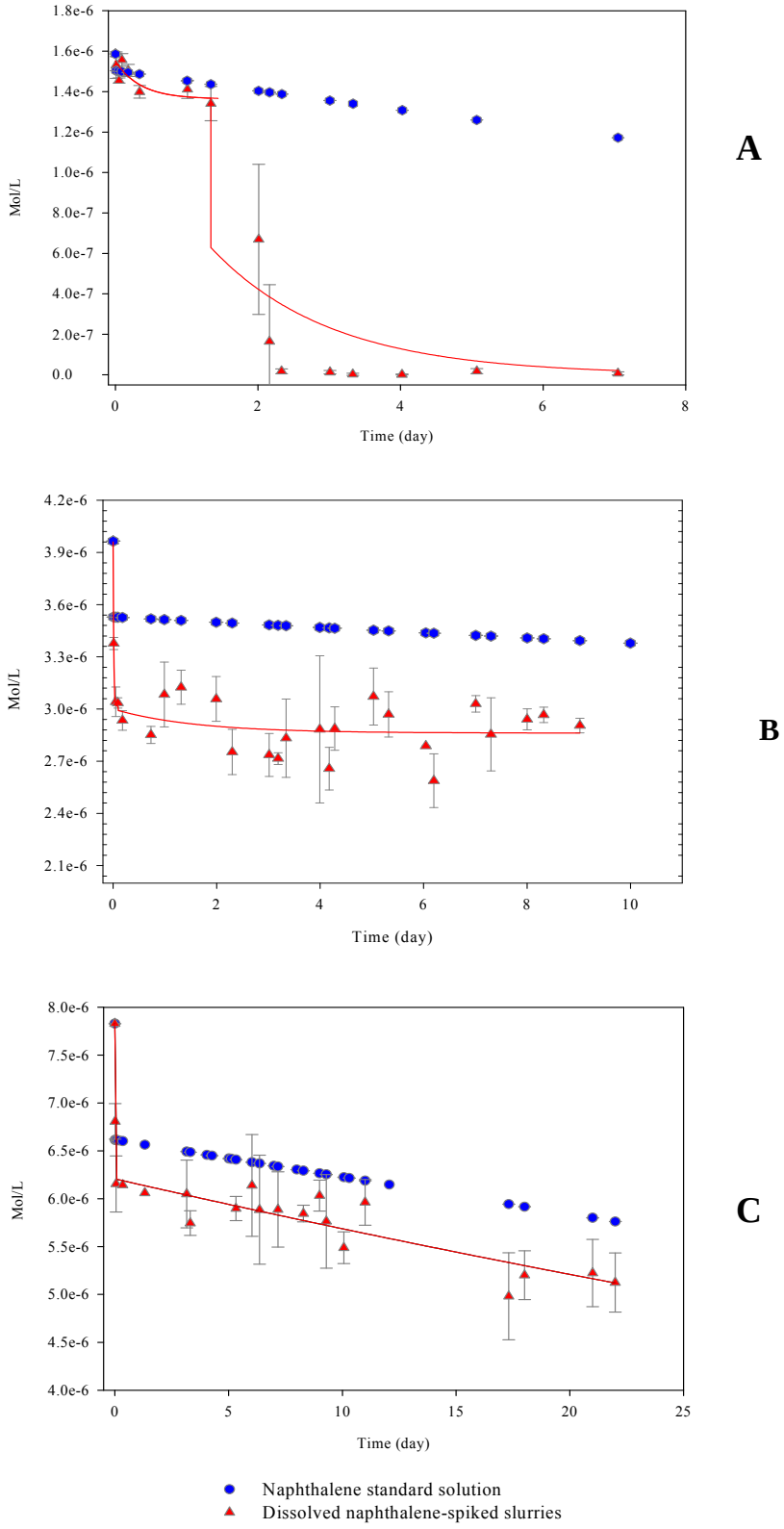

Figure 3.2. Dissolved naphthalene kinetic curves from PACS-2 slurries. Initial naphthalene concentration: (A) 1.6×10^{-6} M, (B) 4.0×10^{-6} M, (C) 7.8×10^{-6} M at 25.0°C. Curve fitted using exponential decay.

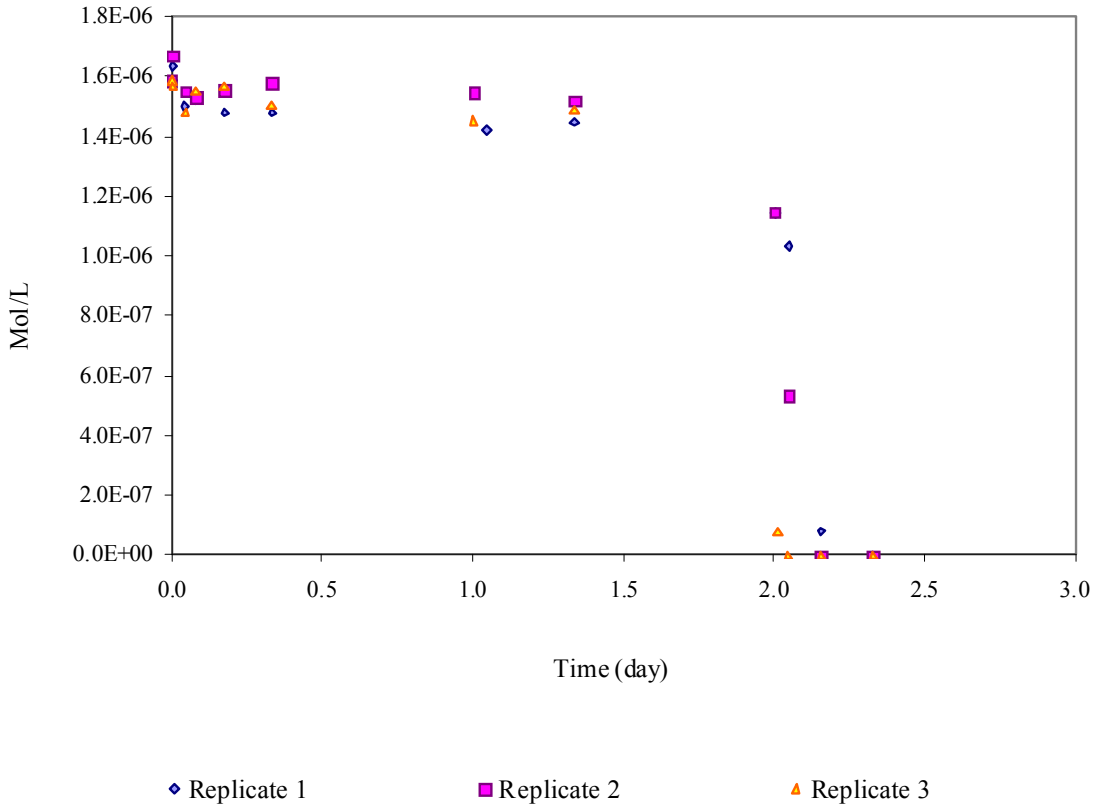

Figure 3.3. Extractable naphthalene concentration curves from triplicates naphthalene-spiked PACS-2 slurries. Initial naphthalene concentration: 1.6×10^{-6} M at 25.0°C. Free-hand curve fitted.

unlikely. There were no visible changes in the physical appearance of the sediments in the slurries that indicated that microbiological activity was occurring. Furthermore Figure 3.3 shows good repeatability between the three replicates. Variable growth rate associated with microorganism and sampling errors (i.e., sub-sampling of sediments) would both affect significantly the repeatability. Possible reasons for the two rapid decrease steps in naphthalene concentration observed in the dissolved and extractable kinetic curves are still unknown.

Results for naphthalene-spiked PACS-2 slurries at 4.0×10^{-6} M (Figures 3.1B and 3.2B) and 7.8×10^{-6} M (Figures 3.1C and 3.2C) show that both extractable and dissolved naphthalene undergo a rapid, early loss in concentration immediately after the beginning of the sorption experiment, which was then followed by a slow, constant decrease in concentration up to the end of the experiments at day 10 and 22, respectively. The observed, early decrease in the naphthalene solution concentration after 24 h in these two experiments (Figs. 3.1B, 3.1C, 3.2B and 3.2C) and in the naphthalene-spiked PACS-2 slurries at 1.6×10^{-6} M (Figs. 3.1A and 3.2A) is consistent with previous observations of sorption kinetics of hydrophobic organic compounds in sediments and soils.[4,9,16,26,27,38,52] For example, it has been observed that the aqueous solution concentration of pyrene, phenanthrene and naphthalene in contact with sediments had significantly decreased after the first few minutes of the beginning of the sorption kinetic experiments. The initial drop in concentration was always followed by a slow decrease of analyte concentration in solution until the equilibrium concentration was reached.[9,16] A similar behavior was observed in a system consisting of atrazine (a pesticide) in contact with clays (e.g., montomorillonite, kaolinite and illite).[38] In this case, both kinetic curves, i.e., extractable and dissolved, showed a fast drop in atrazine concentration within the first day of contact.

This was then followed by a slow decrease in concentration for a period of ~15 days, thereafter the atrazine concentration remained constant for 120 days. The same kinetic behavior was observed for atrazine in contact with a mineral soil (organic carbon content 8.18%)[26] and for the pesticide chlorothalonil in contact with a quartz sand soil (carbon content 1.4%).[52]

3.3.2.1.1 Distribution of Naphthalene in Dissolved and Sorbed States

Kinetic curves for the mass transfer of naphthalene among dissolved, labile sorbed, and bound residue states were calculated from the analysis of the time-dependent concentration curves obtained from online and offline HPLC measurements (as described in Section 2.3.6) for both the naphthalene-spiked PACS-2 slurries and the naphthalene standard solutions (Figures 3.1 and 3.2). Results and discussion of the naphthalene distribution in the dissolved and sorbed states are presented in the following sections.

3.3.2.1.2 Kinetics of Dissolved Naphthalene

Figures 3.2A to 3.2C show the time-dependent concentration curves of dissolved naphthalene derived from naphthalene-spiked PACS-2 slurries having initial naphthalene concentrations (C_0) of 1.6×10^{-6} M, 4.0×10^{-6} M, and 7.8×10^{-6} M, respectively. These curves were used to determine the rate coefficients of naphthalene sorption onto sediment particles. The rate coefficients were calculated using the following integrated rate law expression for a first order reaction:

$$\ln C = \ln C_0 + k_s t \qquad \textbf{(3.1)}$$

where C is naphthalene concentration (mol/L) at any point in time, C_0 is the initial naphthalene concentration (mol/L), k_s is the rate coefficient (day^{-1}) and t is time (day). Figure 3.4 shows the integrated rate law results for PACS-2 slurries having initial naphthalene concentrations (C_0) of $1.6x10^{-6}$ M, $4.0x10^{-6}$ M, and $7.8x10^{-6}$ M. Linear fit of these plots using least squares regressions, gave low correlations coefficients (i.e., $r^2 < 0.5$), hence these fits were not displayed in Fig. 3.4. At least two regions with different slopes can be distinguished in each figure. Since the logarithm operation tends to lessen differences among points and due to the data scattering, difficulties were experienced when trying to determine the regions in which different sorption processes occurred. Therefore, to minimize the uncertainty in the calculations of rate coefficients, curve fitting of the dissolved naphthalene time-dependent concentration curves (Figures 3.2 A-C) was performed instead of the previous integrated rate law method. The direct calculation of the rate coefficients was possible by dividing each kinetic curve in two sections and fitting each section using a curve-fitting program (SigmaPlot v. 8.0). Each section was best described using the following exponential decay equation:

$$C = Y_0 + C_0 e^{-(k_s t)} \qquad \textbf{(3.2)}$$

where Y_0 is the minimum naphthalene concentration reached at the end of each section, and the remaining parameters are the same as in Eq. 3.1. Table 3.2 shows the apparent first order rate coefficients and half-life constants determined for the three initial naphthalene concentrations $1.6x10^{-6}$ M, $4.0x10^{-6}$ M, and $7.8x10^{-6}$ M. The time-dependent concentration curve for dissolved naphthalene in PACS-2 spiked slurries with C_0 equal to $1.6x10^{-6}$ M (Figure 3.2A) underwent an initial, rapid decrease in naphthalene

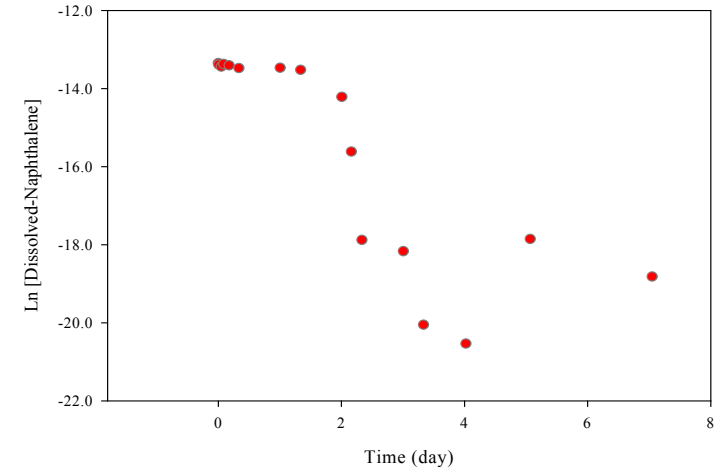

A

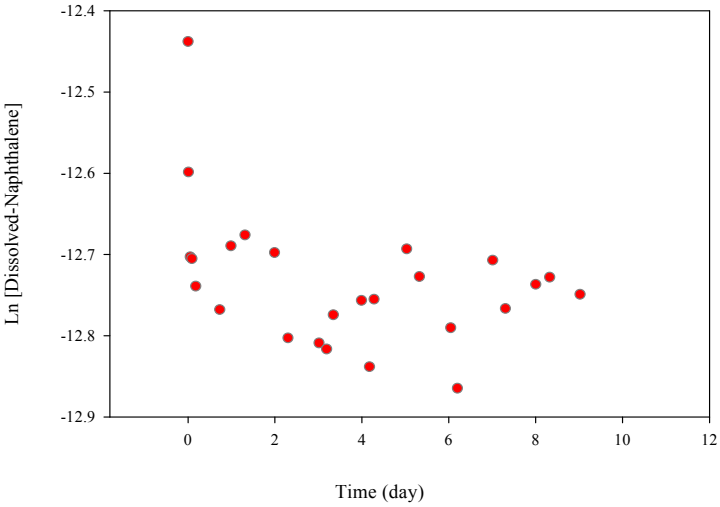

B

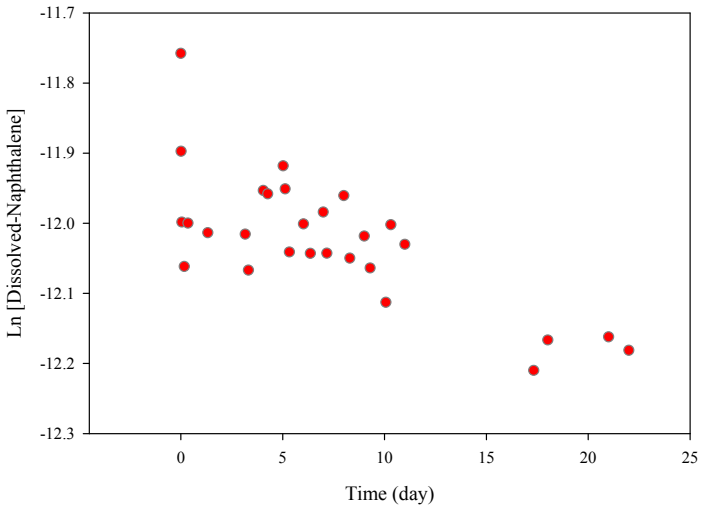

C

Figure 3.4. Natural logarithm of dissolved naphthalene vs. time for PACS-2 slurries. Initial naphthalene concentration: **(A)** 1.6×10^{-6} M, **(B)** 4.0×10^{-6} M, **(C)** 7.8×10^{-6} M at 25.0°C.

Table 3.2. Sorption rate coefficients and half-life constants for apparent first order behavior. PACS-2 naphthalene-spiked slurries at 25.0 °C. Best curve fitting: $C = Y_0 + C_0 e^{-(k_s t)}$

Sorption from Solution Naphthalene (M)	**Duration** day or hour	**Rate Coefficients** k_s day^{-1}	**Stand. Dev.** day^{-1}	**Half-life Constants** $t_{1/2}$ day or hour
1.6×10^{-6}	Day 0 to 1.3 1.3 d = 32 h	3	± 2	0.2 d = 6 h
	Day 1.3 to 7.0 5.7d = 136 h	0.6	± 1	1.2 d = 28 h
4.0×10^{-6}	Day 0 to 2.0 2.0 d = 48 h	92	± 5	0.007 d = 0.2 h
	Day 2.0 to 10 8.0 d = 192 h	0.6	± 2	1.1 d = 26 h
7.8×10^{-6}	Day 0 to 3.2 3.2 d = 77 h	84	± 2	0.3 d = 7 h
	Day 3.2 to 22 19 d = 450 h	0.009	± 0.06	80 d = 1900 h

concentration after 1 hour of contact time that corresponded to a sorption uptake of $1x10^{-7}$ M (3% of initial naphthalene concentration). The calculated rate coefficient for this sorption process was 3 ± 2 day^{-1}. The next 24 hours of the sorption process (day 0.34 to day 1.34) was characterized by a slow, steady decrease of dissolved naphthalene. Six percent of the initial naphthalene concentration was already lost from solution at the onset (day 0.34) of this sorption step. During the subsequent 24 hours of contact time (day 1.34 to day 2.33), the concentration of dissolved naphthalene decreased again rapidly, falling below the limit of detection (LD: $6x10^{-8}$ M) after day 2.34. The calculated rate coefficient was 0.6 ± 1 day^{-1} with a half-life of 28 h.

In the case of naphthalene-spiked PACS-2 slurries with C_0 equal to $4.0x10^{-6}$ M (Fig. 3.2B), curve fitting was done between days 0 to 2.0 and 0.7 to 10. Two pseudo-first order rate coefficients were then determined. Figure 3.2B shows that a rapid decrease in the dissolved naphthalene concentration (14% of initial naphthalene concentration) occurred after 1 hour of contact time. This sorption step lasted 260 minutes (up to day 0.18) and the calculated rate coefficient (k_s) was 92 ± 5 day^{-1} with a half-life of 0.2 h. This sorption process was then followed by a slow, constant decrease in the dissolved naphthalene concentration with a calculated rate constant of 0.6 ± 2 day^{-1} and a half-life of 26 h. The total naphthalene loss from solution after 10 days of contact time was $5x10^{-7}$ M.

The time-dependent concentration curve of naphthalene-spiked PACS-2 slurries with C_0 equal to $7.8x10^{-6}$ M (Figure 3.2C) shows similar features as the naphthalene-spiked PACS-2 slurries with C_0 equal to $4.0x10^{-6}$ M (Figure 3.2B). Fig. 3.2C shows a 7% (i.e., $5x10^{-7}$ M) decrease in the dissolved naphthalene concentration after 1 hour of contact time. This sorption step lasted 490 minutes (up to day 0.34) and the calculated

rate coefficient was 84 ± 2 day^{-1}. A constant, slow decrease in the dissolved naphthalene concentration followed the rapid sorption step and, at the end of the experiment (day 22), a total of $6x10^{-7}$ M (or 11%) naphthalene was removed from solution. The rate coefficient and half-life for this slow sorption process was determined to be 0.009 ± 0.006 day^{-1} and 1900 h, respectively.

The first rate coefficient k_s calculated for the $1.6x10^{-6}$ M naphthalene-spiked slurries was more than thirty times smaller than the first k_s value (see Table 3.2) of the other two naphthalene-spiked slurries (i.e., $4.0x10^{-6}$ M and $7.8x10^{-6}$ M). The reasons for such a difference cannot be attributed to heterogeneity in the composition of the sediment sub-samples used to prepare the slurries, even though the size of sub-samples used in our experiments (i.e., 0.025 g of sediment) was ten times smaller than the minimum sample size required for a representative sample.[46] Good repeatability was obtained generally between replicates of an experiment (see Figure 3.3), which means that sub-sample heterogeneity did not play any significant role.

Rate coefficients and half-life values obtained for the first sorption step are greater by more than one order of magnitude compared to results reported by others researchers for sorption of naphthalene onto sediments. Rate coefficients in the range of 0.07 to 7.4 h^{-1} (or 0.0029 and 0.31 day^{-1}, respectively) and half-life values in the order of 0.09 to 8.7 h^{-1} (or 0.0038 and 0.36 day^{-1}, respectively) have been determined for naphthalene sorption onto sediments. [9,16,21,22]

The large variations in the rate coefficients found in different systems could be due to differences in mole fraction site coverage of the analyte onto the solid. Gamble and Ismaily[38] had observed a strong dependence between the rate coefficients of the

sorption process and the mole fraction coverage. For example, when atrazine was in contact with a mineral soil (8.18% OC), half-life constants of 3.56 to 735 days were found for mole fraction site coverage of atrazine of 0.0199 and 0.95, respectively.

According to equation 1.11, the pseudo-first order rate coefficients obtained can be used along with the labile sorption capacity of the sediment to calculate the second order rate coefficients of the sorption process.[25-29] The determination of the total sorption capacity of the sediments was not carried out due to time limitation. This determination would be necessary in the future to increase the accuracy of mathematical or engineer models used to predict the sorption of contaminants onto soil or sediment particles.[26,27]

3.3.2.1.3 Kinetics of Labile sorbed Naphthalene

Figure 3.5 shows the time-dependent concentration curves of labile sorbed naphthalene at three different initial naphthalene concentrations. The fraction of sorbed naphthalene onto the sediment is characterized in all cases by a transient behavior, i.e., the concentration of labile sorbed naphthalene reaches a maximum and then decreases sometimes to values below the limit of detection. It is also noteworthy to mention that the peak maximum is displaced to longer time as the initial naphthalene concentration is increased.

The time-dependent concentration curve of naphthalene-spiked PACS-2 slurries with C_0 equal to 1.6×10^{-6} M (Figure 3.5 A) shows the formation of a labile sorbed fraction 24 h after the beginning of the sorption kinetic experiment. This fraction reached a maximum at day 2 and was followed by a rapid decrease in naphthalene concentration.

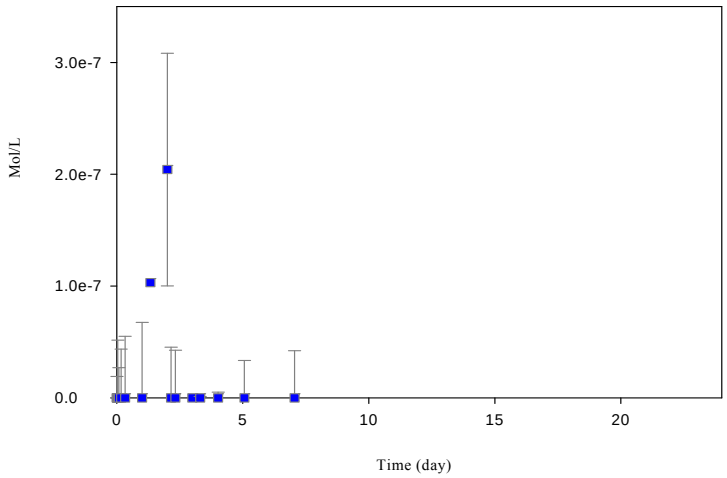

A

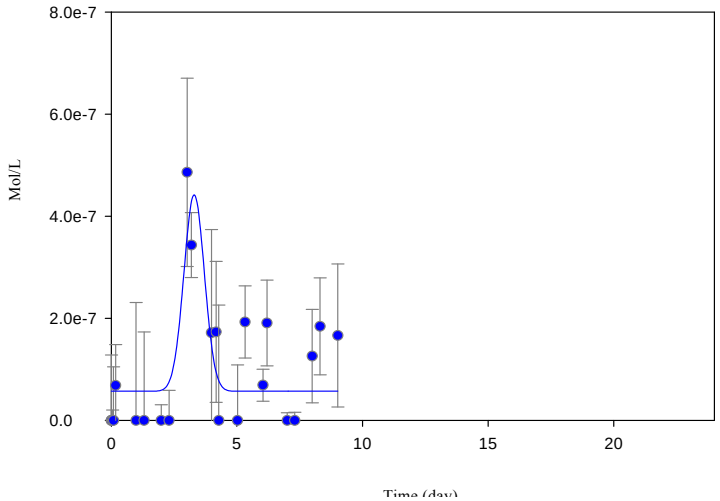

3.1 B

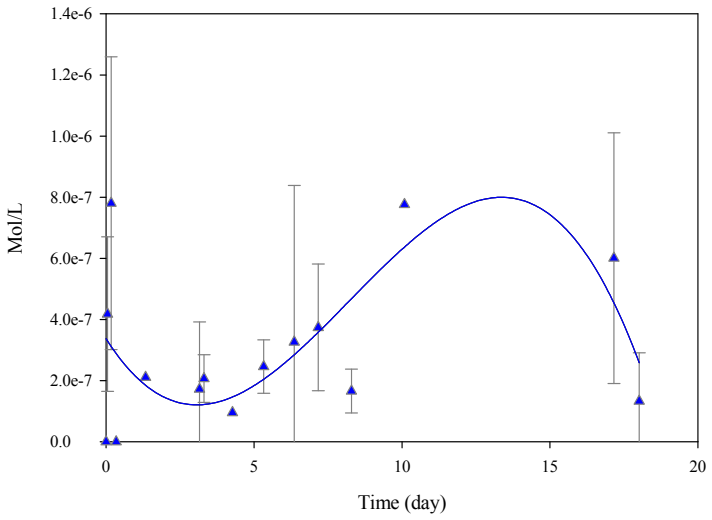

C

Figure 3.5. Labile sorbed naphthalene kinetic curves of PACS-2 slurries. Initial naphthalene concentration: **(A)** 1.6×10^{-6} M, **(B)** 4.0×10^{-6} M, **(C)** 7.8×10^{-6} M at 25.0°C. **(A)** Free-hand curve fitted, **(B)** and **(C)** Curve fitted using least squares regression.

This rapid decay occurred in approximately 1 hour, after which the labile sorbed naphthalene concentration remained below the limit of detection (LD: $6x10^{-8}$ M) for the rest of the experiment. The maximum labile sorbed naphthalene represents 14% of the total naphthalene concentration and corresponds to a loading of 0.23 micro-mol of naphthalene per gram of sediment (i.e., μmol/g of naphthalene onto the sediment).

In the case of naphthalene-spiked PACS-2 slurries with C_0 equal to $4.0x10^{-6}$ M (Figure 3.5B), the transient labile fraction reached a maximum after 3 days of contact time, with a concentration of $0.4x10^{-6}$ M (14% of total naphthalene concentration at day 3), corresponding to a loading of 0.54 μmol/g of naphthalene onto the sediment. After 24 h of reaching this maximum, the labile sorbed fraction decreased to a naphthalene concentration of $0.15x10^{-6}$ M and remained constant at that concentration until the end of the experiment.

Figure 3.5C shows the time-dependent concentration curve of the labile sorbed fraction of naphthalene obtained from the naphthalene-spiked PACS-2 slurries with C_0 equal to $7.8x10^{-6}$ M. A naphthalene labile sorbed fraction was observed 1 h after the beginning of the experiment. The peak maximum appeared between days 10 and 16 and the naphthalene concentration at peak maximum was $0.8x10^{-6}$ M (i.e., 13% of total naphthalene concentration at day 13), which corresponded to a loading of 0.78 μmol/g of naphthalene onto sediment.

The above-mentioned maximum concentration of the naphthalene labile sorbed fraction does not indicate necessarily that the labile sorption sites have been saturated (or all occupied), even if the experimentally determined labile sorption loadings (or capacities) of 0.23 μmol/g, 0.54 μmol/g, and 0.78 μmol/g for initial naphthalene concentration of $1.6x10^{-6}$ M, $4.0x10^{-6}$ M, and $7.8x10^{-6}$ M, respectively, fall within the

range of loading values reported previously by others for pesticides in soils.[4,26,27,34,52] For example, Gamble and co-workers reported labile sorption capacities in the range of 0.37 to 0.67 μmol/g for atrazine in contact with mineral soils (~0.6% organic carbon).[4] On the other hand, when using the same pesticide (atrazine) but in contact with an organic soil, these authors found a labile sorption capacity of 7.0 μmol/g.[34] Similarly, a labile sorption capacity of 28 μmol/g was found for atrazine in contact with humic acids.[34] A literature search yielded no results for naphthalene sorption capacity in sediment slurries.

A comparison of the three naphthalene labile sorbed kinetic curves (Figs. 3.5A to 3.5C) shows that, in addition to the previously mentioned shift of the peak maximum to longer time with increasing initial naphthalene concentration, the total amount of labile sorbed naphthalene (area under the curve) increases non-linearly with initial naphthalene concentration, C_0.

The transient behavior of the labile sorbed fraction observed in our experiments has not been reported before. In sorption kinetic experiments of pesticides onto soils and sediments, the labile sorbed fraction obtained was usually formed within a few hours after the beginning of the sorption experiments and reached a steady concentration after a few days (i.e., 1 to 10 day).[4,26,28] There has been reported cases where a rapid decrease in concentration of this fraction had occurred within the first day. The causes of this phenomenon are not fully understood. It has been attributed to changes in the rate of transfer of the analyte from solution to surface sorption sites and to the formation of a bound residue fraction over time. Initially, the rate of disappearance of analyte from solution to surface sorption sites was considered to be faster than the formation of the bound residue. After some time, this situation changed and the rate of formation of the

bound residue became faster than the rate of disappearance of analyte from solution to the surface sorption sites.[26]

3.3.2.1.4 Kinetics of Naphthalene Bound Residue

Figure 3.6 shows the kinetic curves for naphthalene bound residue at three different initial naphthalene concentrations. For naphthalene-spiked PACS-2 slurries with C_0 equal to $1.6x10^{-6}$ M (Figure 3.6 A), the bound residue fraction obtained after one day of naphthalene in contact with the sediments, was above the limit of detection (LD: $6x10^{-8}$ M) and a maximum concentration of $1.4x10^{-6}$ M was reached at day 2.3. This maximum corresponded to a loading of 1.6 μmol/g of naphthalene onto the sediment.

In this particular case, the bound residue formation was sudden (in less than 17 h) and a diffusion mechanism cannot be invoked to explain its formation. Intraparticle diffusion is a slow process compared to surface sorption.[7,10,45] In general, intraparticle diffusion uses time scales that may range from months to years, whereas surface sorption may be considered as occurring instantaneously i.e., $t << 0.01$ d or, in the range of days.[53] The sudden loss of naphthalene from solution may be attributed to sorption onto new sites of the sediment that became available through the desegregation of the solid particles. Desegregation is most likely due to the breakage of clusters of mineral grains and natural organic matter by the continuous spinning of the slurries.[54] The release of sediment constituents (i.e., natural organic matter) requires a certain amount of time, thus this period may explain the retarded apparition of the bound residue fraction.

Visual inspection of slurries after completion of the sorption experiments showed the formation of two separate fractions of sediment. One fraction tended to accumulate in the upper part of the mixing vessel, whereas the other denser fraction accumulated

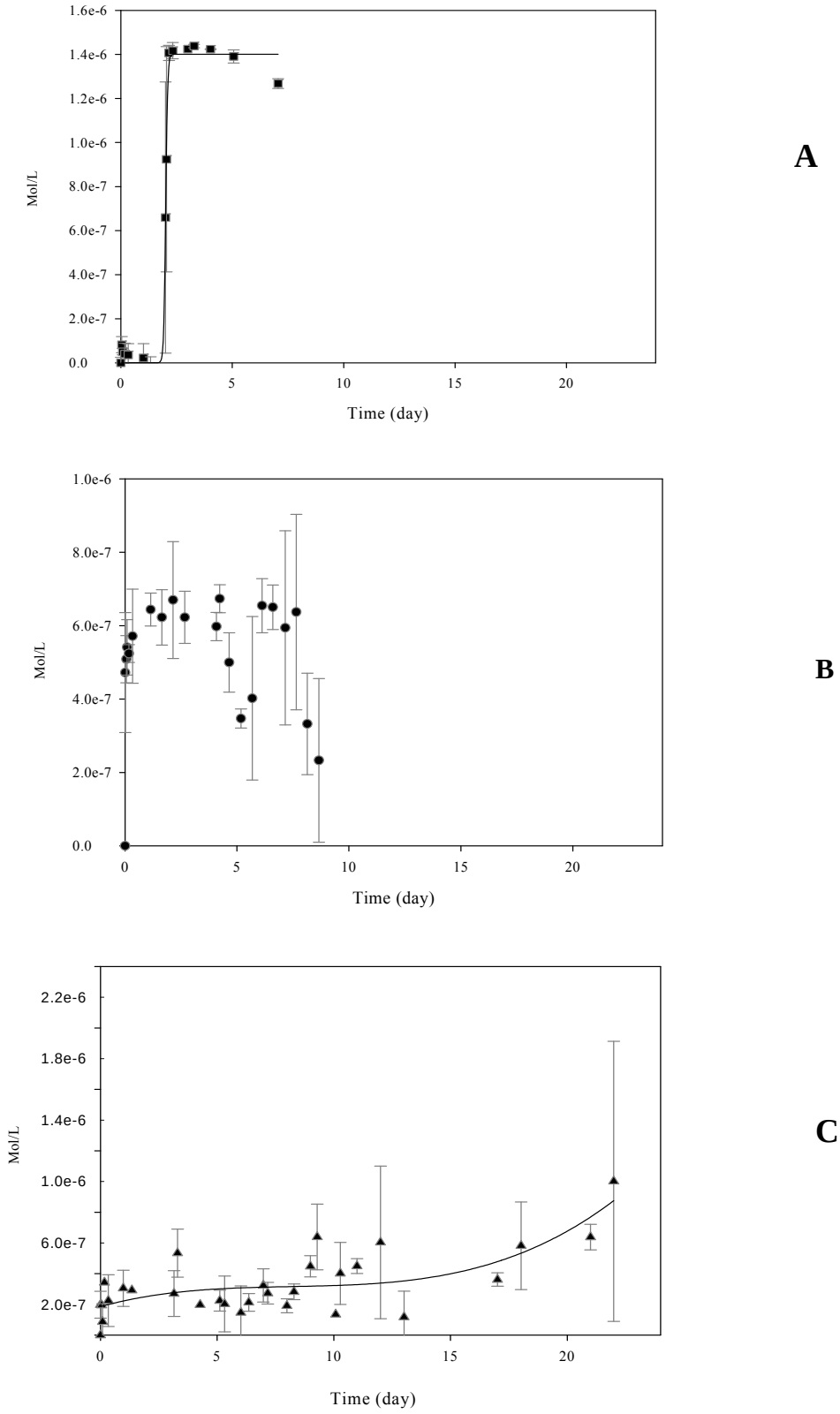

Figure 3.6. Naphthalene bound residue kinetic curves of PACS-2 slurries. Initial naphthalene concentration: **(A)** 1.6×10^{-6} M, **(B)** 4.0×10^{-6} M, **(C)** 7.8×10^{-6} M at 25.0°C. **(A)** and **(C)**: curve fitted using least squares regression, **(B)** free-hand curve fitted.

in the bottom of the vial. Confirmation of the chemical nature of these two fractions would be required in the future to determine whether or not naphthalene has more affinity for a specific fraction.

Ghosh and collaborators[23] in studies of micro-scale location of PAHs in sediments had found that most of the PAHs sorbed were concentrated on the external surface regions of sediments where the organic fraction was mostly localized. Sorption onto this fraction revealed a relatively low PAH availability compare to the PAHs found in the clay/silt fraction.[23]

Figure 3.6B shows the bound residue fraction for naphthalene-spiked PACS-2 slurries with C_0 equal to 4.0×10^{-6} M. This fraction reached a maximum concentration of 6.7×10^{-7} M, (i.e., 18% of total naphthalene concentration) during the second day of the sorption process. The concentration of the naphthalene bound residue then decreased after day 4.2 to reach a minimum of 3.5×10^{-7} M at day 5. The concentration of the naphthalene bound residue increased again and remained relatively constant at 6.6×10^{-7} M between day 6 to day 7.5. The concentration of the naphthalene bound residue finally decreased again to reach a concentration of 2.3×10^{-7} M at day 8.7. The average loading of naphthalene onto non-labile sorption sites of the sediment between day 1 and 9 was in the order of 0.55 ± 0.20 μmol/g.

Figure 3.6C shows the time-dependent curve of naphthalene bound residue fraction for naphthalene-spiked PACS-2 slurries with C_0 equal to 7.8×10^{-6} M. This kinetic curve shows an early formation of the bound residue fraction, reaching a maximum concentration of 3.0×10^{-7} M (i.e., 4% of total naphthalene concentration) at day 1. This concentration remained constant within experimental error up to day 13, and then a slow increase in concentration was observed up to day 22. The final concentration of

bound residue formed was $1.0x10^{-6}$ M, which corresponds to 18% of the initial naphthalene concentration.

Results from the bound residue time-dependent concentration curves (Figs 3.6 A to C) show an inverse dependency between the magnitude of the bound residue and the initial naphthalene concentration. For example, the amount of bound residue at day 7 in the $1.6x10^{-6}$ M naphthalene-spiked slurries was two times greater than in the $4.0x10^{-6}$ M naphthalene-spiked slurries, and five times greater than in the 7.8×10^{-6} M naphthalene-spiked slurries. In contrast with the bound residue, the labile sorbed fraction had a direct dependency with the initial naphthalene concentration (Figures 3.5 A to C). The greatest amount of labile sorbed naphthalene was observed in the sediment slurries spiked to contain $7.8x10^{-6}$ M naphthalene (i.e., the largest initial naphthalene concentration). This is in agreement with a reported study on sorption and desorption kinetic studies of hydrophobic organic compound onto soils and sediments.[55]

3.3.2.2 Desorption Experiments

Desorption experiments were conducted in order to understand better the degree of reversibility of the sorption of naphthalene onto sediments. Test samples for the desorption experiments were prepared by spiking PACS-2 sediment slurries with naphthalene in solution to an initial concentration of $1.6x10^{-6}$ M and $4.0x10^{-6}$ M, as described in Section 2.3.3. The slurries were left in contact with the naphthalene solutions for 8 days ($1.6x10^{-6}$ M) and 12 days ($4.0x10^{-6}$ M) at constant temperature (25.0°C) and with continuous stirring. The liquid and solid phase were then separated by centrifugation and the solid phase was re-suspended using a volume of fresh HPLC grade water that amounted to about 80 to 90% of the original liquid volume of the slurries. This

procedure was repeated several times until the naphthalene concentration in solution was below the limit of detection (LD: $6x10^{-8}$ M). The kinetics of desorption was followed by taking aliquots of slurry over time, and determining the concentration of naphthalene in the sorbed and free states using online microfiltration and offline HPLC separation methodologies.

Figure 3.7A and 3.7B show the time-dependent, concentration curves for naphthalene from naphthalene-spiked PACS-2 slurries with C_0 equal to $1.6x10^{-6}$ M and $4.0x10^{-6}$ M, respectively. These time-dependent, concentration curves showed a fast release of naphthalene during the first three days of the desorption process, reaching a steady concentration at about day 4. For PACS-2 slurries with C_0 equal to $1.6x10^{-6}$ M, 6% of the initial naphthalene concentration was obtained after 15 days of the desorption process. This fraction corresponded to a loading of 0.11 ± 0.04 μmol/g of naphthalene onto the sediment. In the case of PACS-2 slurries with C_0 equal to $4.0 x10^{-6}$ M, 8% of the initial naphthalene concentration was found in solution after 14 days of the desorption. This fraction corresponded to a loading of 0.35 ± 0.01 μmol/g of naphthalene onto the sediment. Kan and collaborators reported comparable results for naphthalene desorption from mineral soils, in which 11% to 37% of the total naphthalene sorbed was recovered 7 days after initiating the desorption process.[9]

Rate coefficients for the desorption of naphthalene were calculated from the time-dependent concentration data measured using the offline HPLC methodology, since there were no significant differences between the online and offline HPLC kinetic curves (Figures 3.7A and B). The first order rate coefficients were calculated using the same systematic approach used before for naphthalene sorption. This procedure was used because poor linear regression fits (i.e., low correlation coefficient) were obtained for the

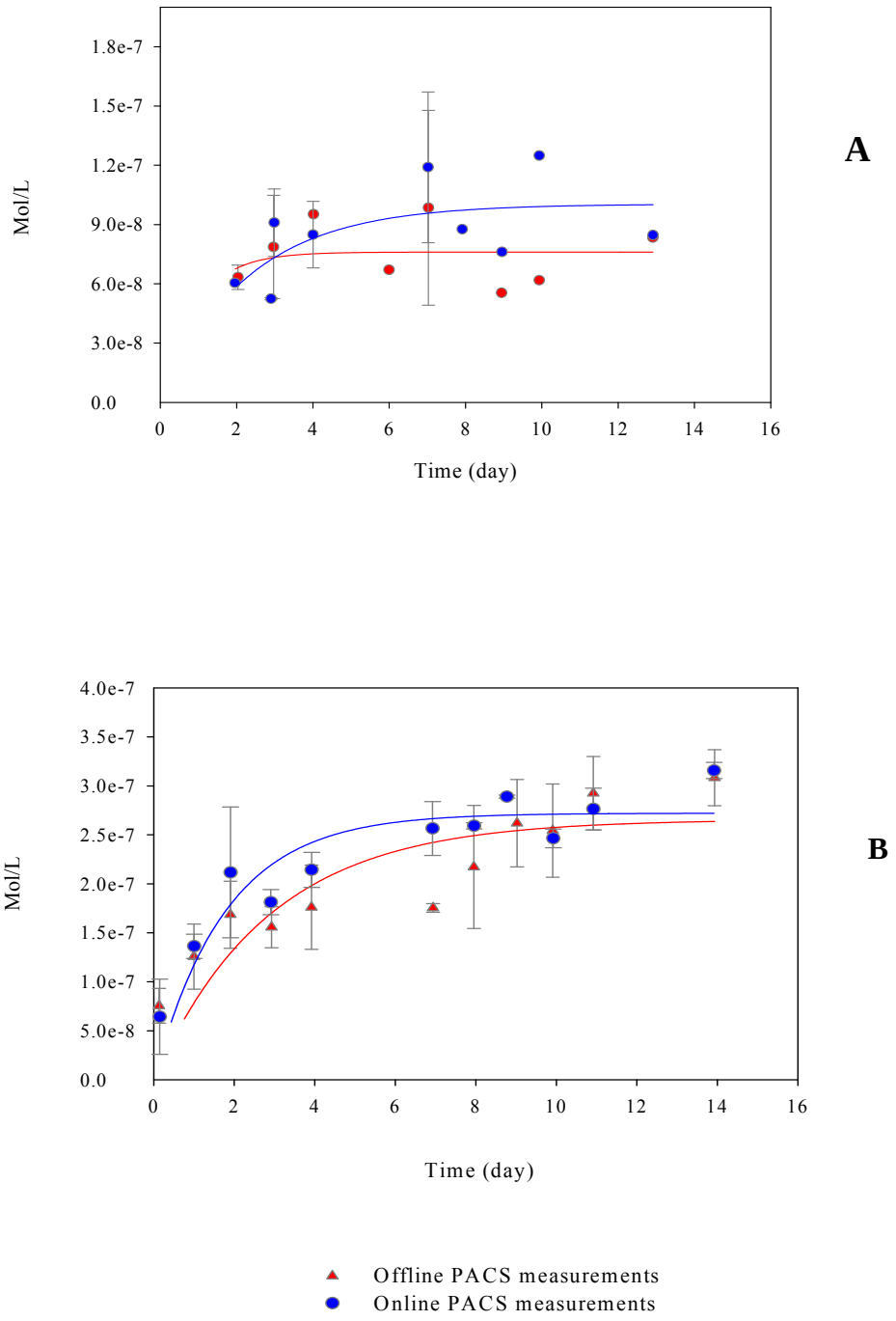

Figure 3.7. Naphthalene desorption kinetic curves of PACS-2 slurries. Initial naphthalene concentration: **(A)** 1.6×10^{-6} M, **(B)** 4.0×10^{-6} M at 25.0°C. Curve fitting using exponential rise.

plots of natural logarithm of desorbed naphthalene versus time (see Figures 3.8A and B) and also because it ensured consistency in the data treatment. A different exponential expression was used to calculate the sorption rate coefficient. The entire data set was best fitted using a single exponential rise expression of the form shown in Equation 3.3:

$$C = X_0 (1 - e^{-(k_s t)}) \qquad \textbf{(3.3)}$$

where X_0 is the concentration in mol/L of naphthalene reversibly sorbed onto sediment particles and the remaining parameters are the same as in Eq. 3.1. Table 3.3 shows the apparent first order rate coefficients and half-life constants obtained for naphthalene desorption at 1.6×10^{-6} M and 4.0×10^{-6} M.

There are significant differences among reported values of half-life constants and rate coefficients for the desorption of naphthalene from soils and sediments. For example, Kan and collaborators reported half-life constants in the order of 22 to 65 days, calculated using the same mathematical approximation adopted here.[9] Karickhoff[16] and, Wu and Gschwend[21] had reported half-life constants for naphthalene desorption from sediments in the range of 0.07 to 1.14 h. In this study, the calculated half life values for the desorption of naphthalene from spiked slurries at 1.6×10^{-6} M and 4.0×10^{-6} M were 1.6 and 1.2 day, respectively.

The differences between the rate coefficients determined in this work and those reported by other investigators may be attributed to several experimental variables that can affect the fraction of hydrophobic organic compounds sorbed or released from a geosorbent. For example, the time of the analyte in contact with the solid has been established to have an important incidence in the site coverage of the solid and in the size

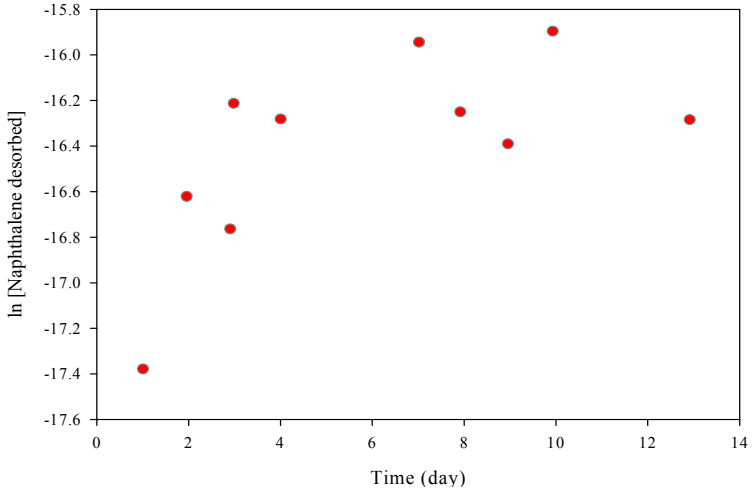

A

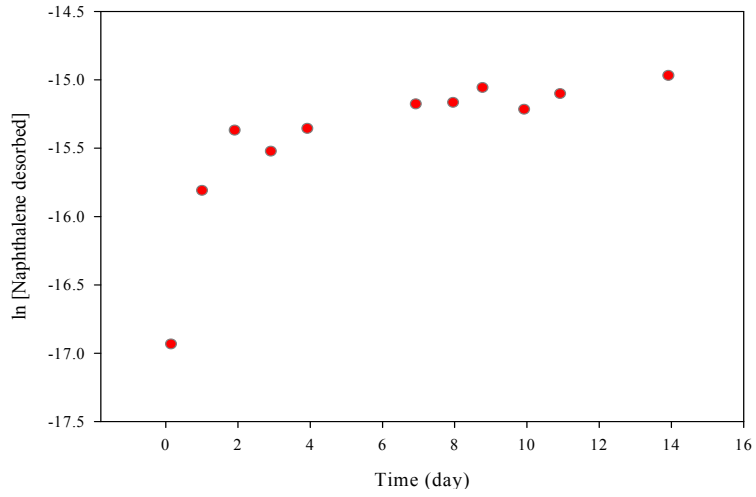

B

Figure 3.8. Natural logarithm of the concentration of desorbed naphthalene vs. time for PACS-2 slurries. Initial naphthalene concentration: **(A)** 1.6×10^{-6} M, **(B)** 4.0×10^{-6} M at 25.0°C.

Table 3.3. Desorption rate coefficients and half-life constants for apparent first order behavior. PACS-2 naphthalene-spiked slurries at 25.0°C. Best curve fitting desorption: $C = X_0 (1- e^{(-k_s t)})$

Initial naphthalene concentration (M)	Duration day or hour	Rate Coefficients k_s day^{-1}	Stand. Dev. day^{-1}	Half-life Constants $t_{1/2}$ day or hour
$1.6x10^{-6}$	Day 0 to 13 13 d = 322 h	0.4	± 0.1	1.6 d = 38 h
$4.0x10^{-6}$	Day 0 to 14 14 d = 336 h	0.6	± 0.1	1.2 d = 30 h

of the fraction sorbed and released from the solid.[9,16,38,55-58] Kan and collaborators[9] observed that the amount of naphthalene released from freshly spiked sediment slurries decreased by 23% to 15% when the contact time was increased from 1 to 30 days, respectively. The same behavior was reported by Karickhoff[16] in a study of pyrene in contact with sediments. In this case the fraction released from the sediment was reduced from 0.99 to 0.070 when the incubation time increased from 4 min to 122 h, respectively. In that system 36% of sorbed pyrene was recovered after 122 h of incubation.

Gamble and collaborators[38] showed that the sorption/desorption rate coefficient depends strongly on the mole fraction site coverage of the solid. In the case of the pesticide atrazine sorbed onto a mineral sediment (8.18% OC), the rate coefficients for the desorption process changed from days 1.03 to 10.9 when the mole fraction site coverage was increased from 0.0199 to 0.95, respectively.

Other experimental variables such as the presence of co-solutes can affect the rates of sorption and desorption.[59,60] White and Pignatello[60] found that the rate of desorption of phenanthrene increased when pyrene was presented. Phenanthrene desorption rates without the presence of pyrene were in the order of 0.394 and 1.04 d^{-1} for a sandy loam (1.4% OC) and a peat soil (43.9% OC), respectively. These rates of desorption, after a short uptake period (2 days), increased to 0.838 and 1.59 day^{-1} when pyrene concentration was increased to 2850 and 4840 μg of pyrene per gram of soil, respectively. These researchers also observed the same behavior when a longer term experiment (i.e., 42 and 76 days) was conducted with the two above-mentioned soils. In this case, the rate coefficients increased by a factor of ~1.5, when pyrene concentration increased to 1010 μg of pyrene per gram of loam and 690 μg of pyrene per gram of peat.[60]

The pre-treatment of the solids, prior to being spiked with the analyte of interest, can affect the sorption and desorption processes. For example, alterations of the original composition and morphology of the solid can occur depending on the procedure used for storage (i.e., temperature and length of storage), to handle the solid (i.e., procedures to mix, sieve, dry and rewet the solid), or to keep the slurry in uniform suspension in the mixing vessels. [50,54]

The procedure used to put the analyte in contact with the solid is also a factor that may alter the sorption and desorption processes. Spiking procedures can be performed using wet or dry solids with aqueous or organic solvents. The use of wet or dry solids can affect the uniformity in which the organic contaminant is distributed. The presence of co-solvents (used to introduce the organic compound in solution) can increase the total fraction of organic compound in the solid, depending of their persistence in solution.[50]

Finally, comparable desorption rate coefficients have been obtained using different analytical techniques (e.g. batch and miscible displacement techniques). It is important to note however that similar time scales must be used when comparing rate coefficients determined using different analytical techniques.[61]

3.3.3 HISS-1 Sediment

The second system studied was the marine sediment HISS-1 spiked with naphthalene to an initial concentration of 1.6×10^{-6} M. Other initial naphthalene concentrations were not studied because of time limitation. HISS-1 sediment is different from PACS-2 sediment in the following ways: HISS-1 sediment present lower carbon content (i.e., 10 fold smaller than PACS-2), and has a mineral composition mainly comprised of quartz (99.4 %) and a small amount of halite (0.6% NaCl). More details on the composition of HISS-1 are given in Table 3.1. The experimental conditions for the sorption and desorption experiments were the same as described previously for PACS-2 slurries in Section 3.3.2.1 and 3.3.2.2, respectively.

3.3.3.1 Sorption Experiments

Figures 3.9A and 3.9B show the dissolved and extractable naphthalene kinetic curves for the naphthalene-spiked HISS-1 slurries, respectively, at an initial naphthalene concentration of 1.6×10^{-6} M. The time-dependent concentration curve for a naphthalene standard solution, having the same initial naphthalene concentration as the slurries, was included with each kinetic curve for comparison purposes.

Both dissolved and extractable kinetic curves showed a rapid, early loss in naphthalene concentration during the first day of the sorption experiment. This rapid decrease in naphthalene concentration was followed by a slow, constant decrease in concentration for the remainder of the experiment (i.e., day 17). These sorption kinetic results are comparable to those reported for naphthalene in contact with PACS-2 sediment (see previous section), and are in agreement with those reported by other groups for the sorption of hydrophobic organic compounds onto soils and sediments.[4,9,16,26,38,45]

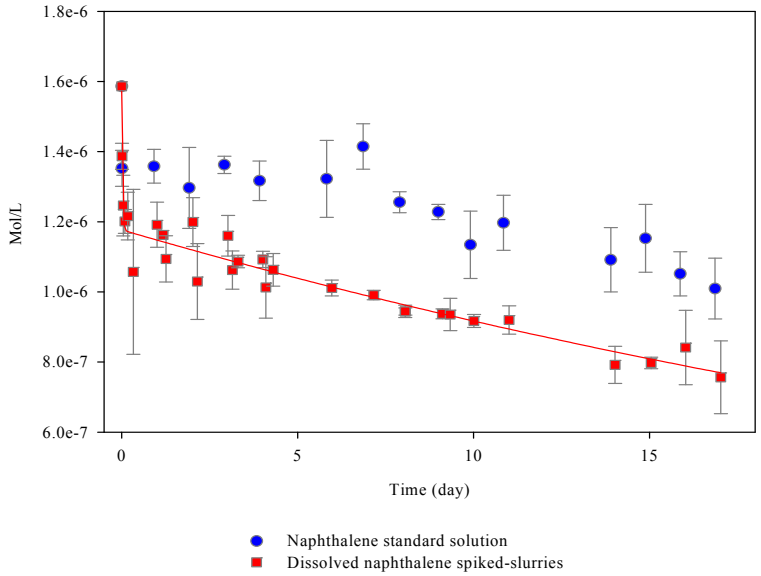

A

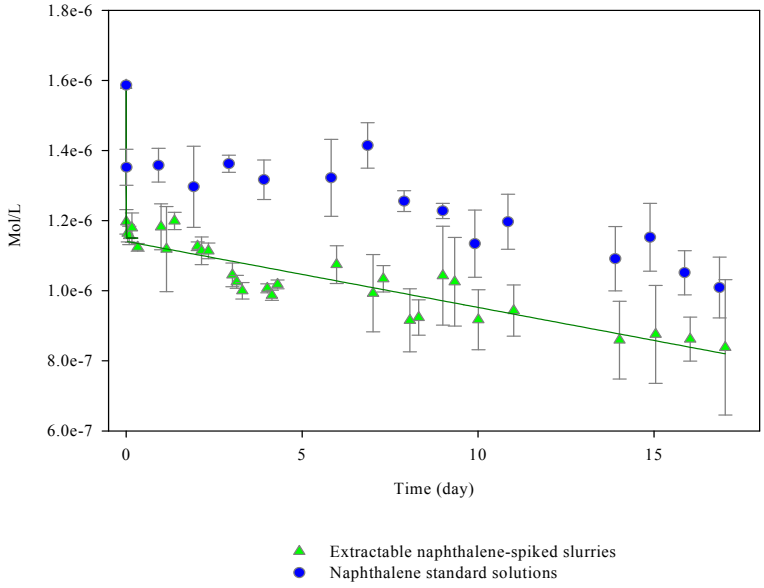

B

Figure 3.9. Dissolved and extractable naphthalene kinetic curves of HISS-1 slurries. Initial naphthalene concentration 1.6×10^{-6} M at 25.0°C. **(A)** Dissolved naphthalene, **(B)** Extractable naphthalene. Curve fitted using least square regression (naphthalene standard) and exponential decay (naphthalene-spiked slurries).

3.3.3.1.1 Distribution of Naphthalene in Dissolved and Sorbed States

Kinetic curves for the mass transfer of naphthalene between the dissolved, labile sorbed, and bound residue states were calculated from the analysis of the time-dependent concentration curves of naphthalene-spiked HISS-1 slurries and naphthalene standard solutions obtained from online and offline HPLC measurements (Figures 3.9A and 3.9B), as described in Section 2.3.6.

Figure 3.10 shows the time-dependent concentration curves for dissolved, labile sorbed and bound residue fractions of naphthalene-spiked HISS-1 slurries with C_0 equal to 1.6×10^{-6} M. The kinetic curve for dissolved naphthalene (triangle symbol) shows an early, fast decrease in naphthalene concentration. Approximately 12% of the initial naphthalene concentration was lost from solution after two hours of contact. This corresponded to a loading of 0.19 μmol/g of naphthalene sorbed onto the sediment. This early drop in concentration was followed by a slower steady decrease and, by day 17, the initial naphthalene concentration was reduced by 29% (i.e., 0.35 μmol/g of naphthalene sorbed onto the sediment).

Figure 3.10 also shows the time-dependent concentration curve for labile sorbed naphthalene (circle symbol). Unlike naphthalene in contact with PACS-2 sediment, no transient fraction of labile sorbed naphthalene was observed. In the case of naphthalene in contact with HISS-1 sediment, the concentration of naphthalene oscillated between 0.7×10^{-7} to 1.6×10^{-7} M for most of the experiment (i.e., from day 3 to 17), and this corresponded to an average loading of 0.10 to 0.18 μmol/g of naphthalene onto the sediment, respectively.

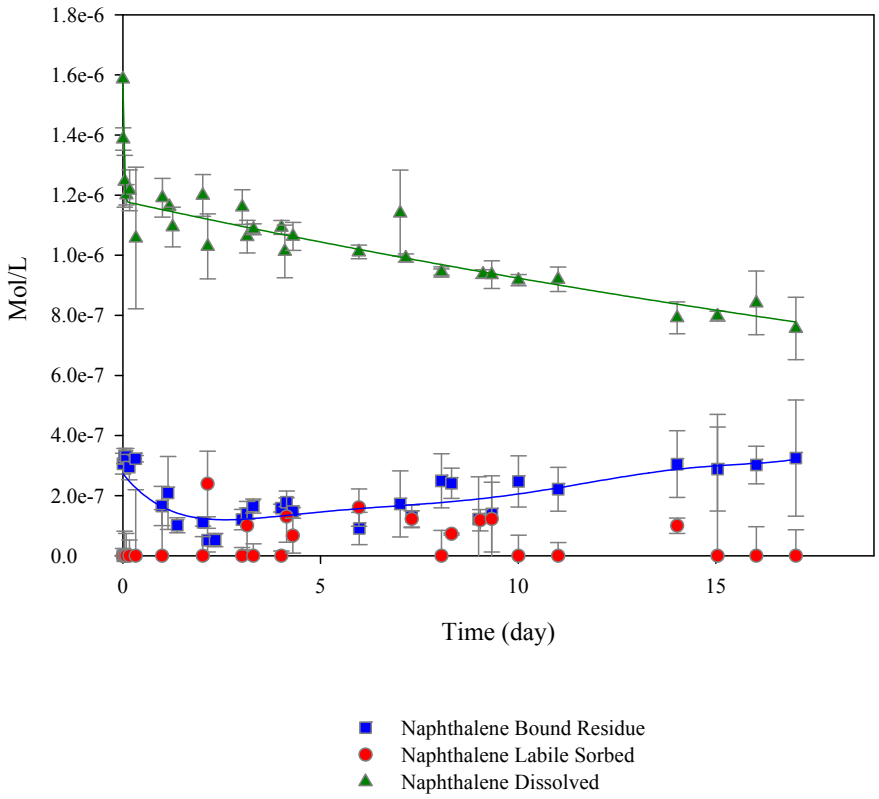

Figure 3.10. Dissolved, labile sorbed and bound residue naphthalene kinetic curves for HISS-1 slurries. Initial naphthalene concentration 1.6×10^{-6} M at 25.0°C. Dissolved naphthalene curve was fitted using exponential decay, labile sorbed naphthalene was free hand curve fitted, and bound residue naphthalene curve was fitted using least square regression.

The time-dependent concentration curve of naphthalene bound residue is also shown in Figure 3.10. This fraction was observable immediately after the beginning of the experiment. After 8 hours into the sorption process, a concentration of $3x10^{-7}$ M was reached. The naphthalene bound residue concentration then reached a minimum concentration of 1 x 10^{-7} M at day 2.3. After day 2.3, the bound residue concentration increased slowly up to a concentration of $3x10^{-7}$ M by day 17. This concentration corresponded to a loading of 0.4 μmol/g of naphthalene sorbed onto the sediment. It is interesting to note that from day 2 and onward, the rate of loss of dissolved naphthalene is approximately equaled to the rate of formation of naphthalene bound residue.

3.3.3.1.2 Kinetics of Dissolved Naphthalene

Pseudo-first order rate coefficients of naphthalene sorption were calculated in the same fashion as for the naphthalene - PACS-2 sediment slurries (see section 3.3.2.1.2). They were obtained directly from curve fitting the time-dependent concentration curve of dissolved naphthalene (Figure 3.10). Figure 3.11 shows a plot of natural logarithm of dissolved naphthalene concentration versus time. Two linear sections, between day 0 and day 1.3 and between day 1.3 and day 17, can be distinguished from the time-dependent logarithmic concentration curve. In order to maintain consistency in the data treatment, an exponential decay fit was used instead of a linear regression fit to determine the rate constant of each linear portion of the curve.

The dissolved naphthalene kinetic curve was divided into two sections (day 0 to day 1.3, and day 1.3 to day 17) and each section was fitted using Eq. 3.2 (fit curve not shown). Table 3.4 shows the calculated apparent first order rate coefficients and half-life constants for each section. The naphthalene sorption rate coefficient for the time period

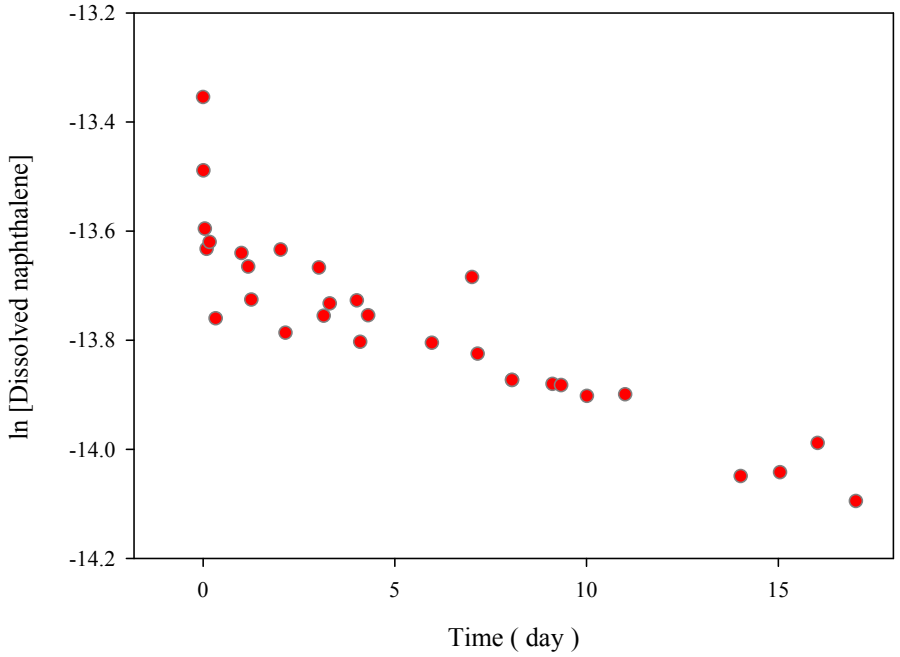

Figure 3.11. Natural logarithm of the dissolved naphthalene concentration vs. time for HISS-1 slurries. Initial naphthalene concentration 1.6×10^{-6} M at 25.0°C.

Table 3.4. Naphthalene sorption and desorption rate coefficients and half-life estimates for apparent first order behavior for HISS-1 slurries. Initial naphthalene concentration: 1.6×10^{-6} M at 25.0 °C. Best curve fit: Sorption: $C = C_0 e^{-(k_s t)}$ Desorption: $C = X_0 (1 - e^{-(k_s t)})$

Process	**Duration**	**Rate Coefficients**	**Stand. Dev**	**Half-life Constants**
	day or hour	**k_s day^{-1}**	**day^{-1}**	**$t_{1/2}$ day or hour**
Sorption	Day 0 to 1.3 1.3 d = 32 h	33	± 3	0.02 d = 0.5 h
	Day 1.3 to 17 16 d = 380 h	0.02	± 0.04	28 d = 670 h
Desorption	Day 0 to 17 17 d = 410 h	0.5	± 0.3	1.3 d = 30 h

day 0 to day 1.3 is ten times larger for the HISS-1 sediment system compared to the PACS-2 sediment system for the same initial naphthalene concentration of $1.6x10^{-6}$ M. On the other hand, the sorption rate coefficient for subsequent time period, i.e., day 1.3 to end of experiment (i.e, day 7 for PACS-2 and 17 for HISS-1), is 30 times smaller for the HISS-1 sediment system compared to the PACS-2 sediment system.

3.3.3.2 Desorption Experiments

The naphthalene-spiked HISS-1 slurries were prepared as described previously in section 3.3.2.2, with the exception that HISS-1 sediment was used instead of PACS-2 sediment. Also, curve-fitting procedure using Eq. 3.3 and data treatment are consistent with the procedure used in section 3.3.2.2.

Figure 3.12 shows the time-dependent concentration curves for the desorption of naphthalene from a naphthalene-spiked HISS-1 slurries with C_0 equal to $1.6x10^{-6}$ M using online and offline HPLC methodologies. There are no differences between these two kinetic curves (i.e., online and offline) within experimental errors. In each case, the naphthalene concentration increased exponentially until it reached a constant value at day 4. About 8% of the initial naphthalene concentration was released to solution after 13 days of desorption.

The desorption rate coefficient for naphthalene was calculated using the time-dependent concentration data measured using offline HPLC methodology. A rate coefficient value of 0.5 d^{-1} was obtained (Table 3.4). This rate coefficient is comparable to the rate obtained for the desorption of naphthalene from PACS-2 sediments with C_0 equal to $1.6x10^{-6}$ M and $4.0x10^{-6}$ M.

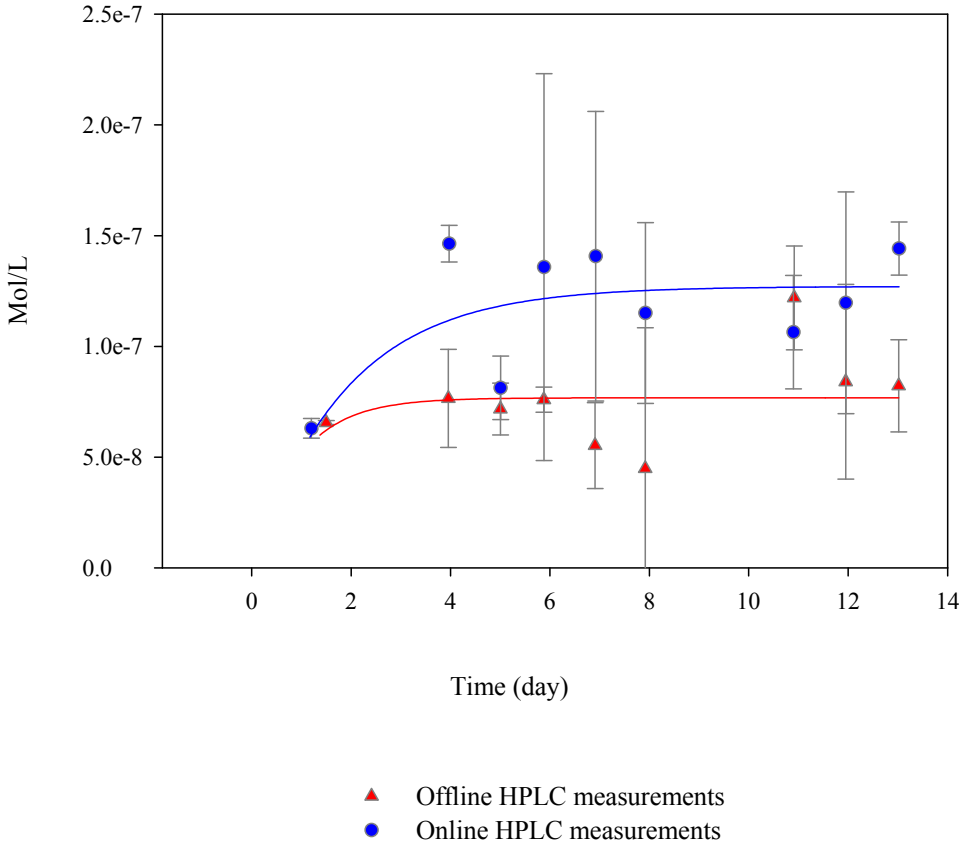

Figure 3.12. Naphthalene desorption kinetic curves of HISS-1 slurries. Initial naphthalene concentration 1.6×10^{-6} M at 25.0 °C. Curve fitted using exponential rise.

3.3.4 PACS-2 and HISS-1 Sediments

3.3.4.1 Unknown Chromatographic Peak

An unknown, well-resolved chromatographic peak was observed in the analysis of sediment slurries. This chromatographic signal was consistently observed in the chromatogram of the solution obtained from the online microfiltration and offline centrifugation analysis of the PACS-2 and HISS-1 slurries spiked at different naphthalene concentrations. The chromatographic peak was also observed in the sediment blank and naphthalene standard solutions.

Figure 3.13 shows a typical chromatogram for the online microfiltration or offline centrifugation analysis of either naphthalene-spiked PACS-2 or HISS-1 slurries. An unknown chromatographic peak with a retention time of about 0.94 min was observed prior of the appearance of the dissolved naphthalene peak (retention time of about 2.0 min.) during the offline centrifugation analysis of a naphthalene-spiked PACS-2 slurry that had an initial naphthalene concentration of 4.0×10^{-6} M. Figure 3.14A, B, and C show the time-dependent concentration curves of the formation of this unknown in a naphthalene-spiked PACS-2 slurry that had an initial naphthalene concentration of 1.6×10^{-6}, 4.0×10^{-6}, and 7.8×10^{-6} M, respectively. Since there is no analytical chemical standard for this unexpected peak, there is no correction for variability in the instrument response. Nevertheless, a general trend for the formation of this unknown peak in naphthalene-spiked PACS-2 slurries could be observed. In general, Fig. 3.14A to C show that this unknown peak reached a maximum about 2.5 to 4 days after the beginning of the sorption experiment. A rate coefficient of 0.3 day^{-1} was calculated for the formation of

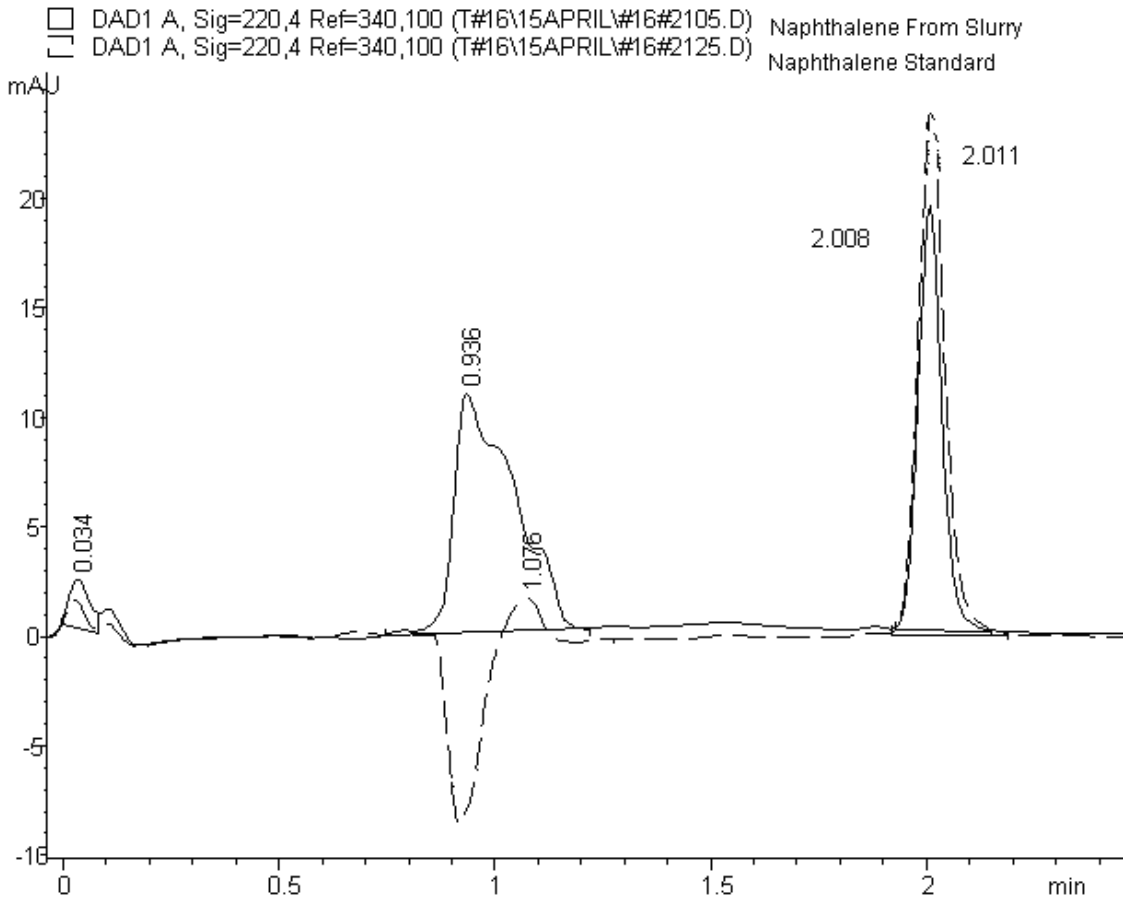

Figure 3.13. HPLC peaks of naphthalene and unknown peak. Aliquot offline centrifuged from 4.0×10^{-6} M naphthalene-spiked PACS-2 slurry at contact time t = 6.2 day. Retention times: naphthalene: 2.0 min, unknown peak: 0.94 min. Dashed line: naphthalene standard, full line: naphthalene from slurry.

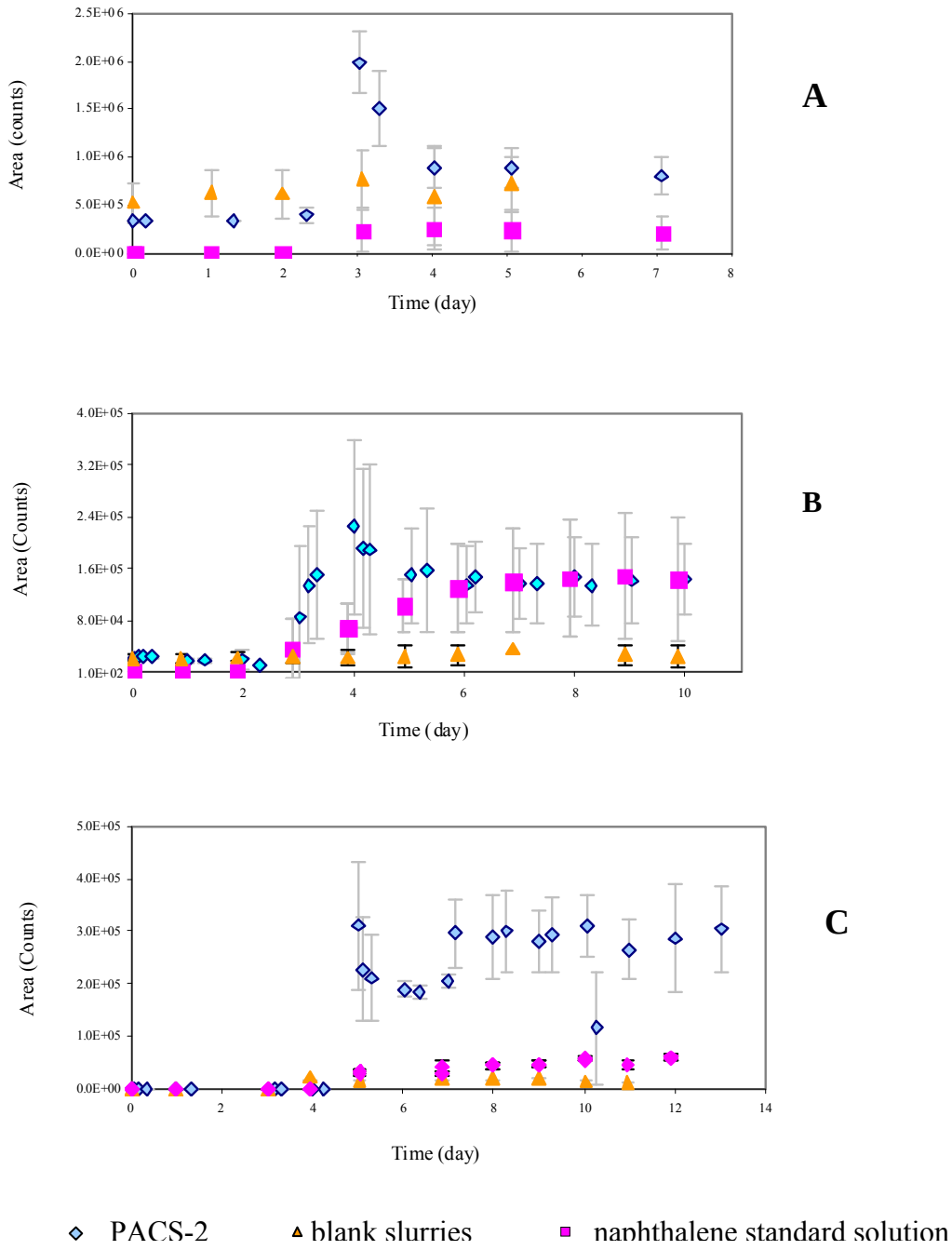

Figure 3.14. Time-dependent curves for the detection of unknown peak at λ 220nm in naphthalene-spiked slurries, blank slurries and naphthalene standard solutions at **(A)** 1.6×10^{-6} M, **(B)** 4.0×10^{-6} M and **(C)** 7.8×10^{-6} M.

this peak assuming a first order reaction behavior. The unknown peak was also observed during the desorption experiments but no rate constant for the formation of this peak was calculated.

The unknown peak was also observed in the case of naphthalene-spiked slurries HISS-1. In this case, the formation of the unknown peak reached a maximum three days after the beginning of the sorption experiment, which is similar to the above-mentioned result for naphthalene-spiked PACS-2 slurries.

Figure 3.15A, 3.15B. and 3.15C show a chromatogram that include the unknown and naphthalene peaks, the real time UV spectrum of the unknown peak, and the real time UV spectrum of the naphthalene peak taken from a naphthalene-spiked PACS-2 slurries, respectively. The real time UV spectrum is obtained directly from the HPLC PhotoDiode Array (PDA) detector. The initial naphthalene concentration was 7.8×10^{-6} M and the supernatant solution was analyzed using the offline centrifugation HPLC technique. A library search using the photodiode array detector library found no match for the spectrum of the unknown peak.

A preliminary chemical analysis of this peak was performed using an high performance liquid chromatography mass spectrometry, HPLC-MS, technique.[62,63] Atmospheric-pressure chemical ionization, APCI, source [HP G1947A, Agilent Technologies] was used as the ion source interface between the HPLC and MS systems [HP 1100 Series, Agilent Technologies].

Optimization of the MS was performed using direct infusion of naphthalene standard solutions at a flow rate of 600 μL/h. Details of the experimental parameters used in the HPLC-APCI-MS analysis are given in Appendix 3. A limit of detection of

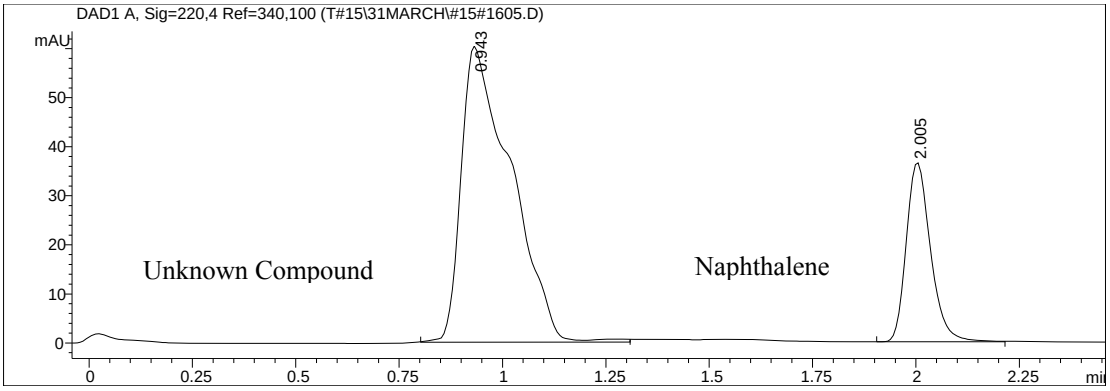

A

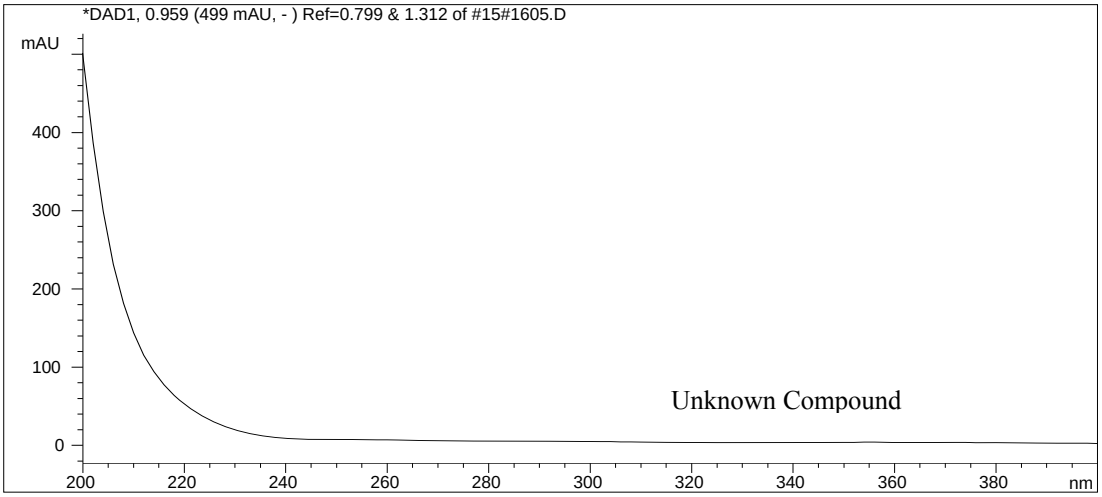

B

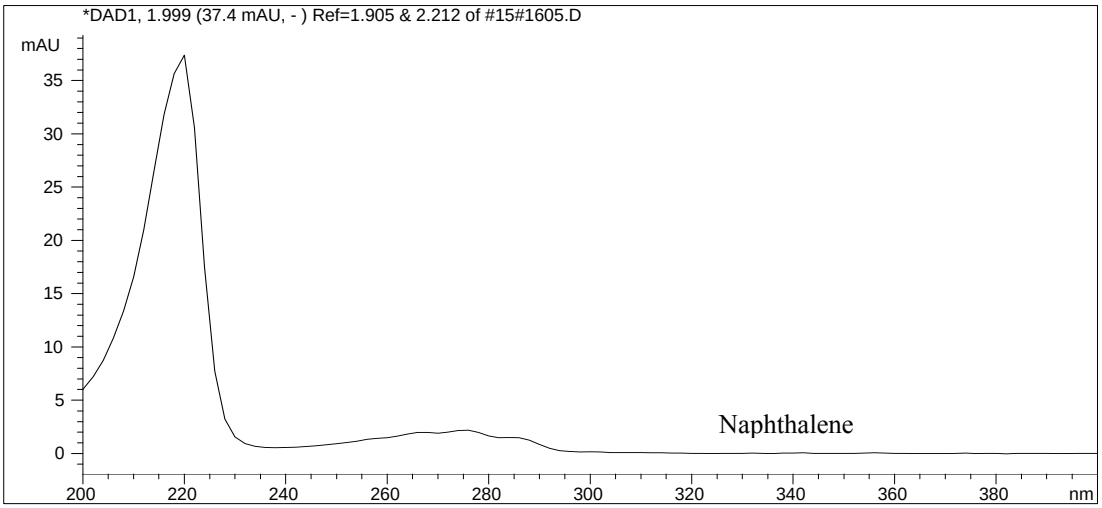

C

Figure 3.15. HPLC peaks and UV spectra of naphthalene and unknown. **(A)** aliquot offline centrifuged from 7.8×10^{-6} M naphthalene-spiked PACS-2 slurry at contact time t = 6.0 day. Retention time (r_t): naphthalene: 2.01 min; unknown peak: 0.94 min. **(B)** UV spectrum of unknown compound r_t = 0.96 min. **(C)** UV spectrum of naphthalene r_t = 1.99 min.

$7.8x10^{-5}$ M was determined. Unfortunately, the MS limit of detection for naphthalene was significantly larger than the concentration used in the experiments of this study. Therefore, detection of naphthalene and structure or chemical identification of the unknown peak could not be accomplished. It is believed that the origin of this peak is related to the injection of samples onto the HPLC and their UV detection. When an injection is performed, a plug of sample solution enters the HPLC and the solvent of the sample, (i.e. 2% acetonitrile) which is not retained in the chromatographic column, passes to the detection cell changing momentarily the composition of the mobile phase and therefore generating an absorbance signal. This may explain why this unknown chromatographic signal is observed in samples of blank slurries, naphthalene spiked-slurries, and naphthalene standard solutions. It is relatively improbable that this peak would be a secondary reaction by-product of naphthalene or a sub-product of the sediment (e.g., leach out product).

3.3.4.2 Kinetics of Sorption

Figures 3.16A to 3.16C show the naphthalene distribution among solution, labile sorbed, and bound residue fractions for PACS-2 and HISS-1 spiked with $1.6x10^{-6}$ M naphthalene. Figures 3.16A to C are constructed from parts of Figures 3.2A, 3.5A, 3.6A, and 3.10. Dissolved and bound residue kinetic curves (Figures 3.16A and 3.16C, respectively) differ greatly between the two sediments. The time-dependent concentration curve of the dissolved naphthalene for HISS-1 slurries shows a constant decrease in naphthalene concentration over time, and no sudden naphthalene loss was observed at day 2 as observed in the case of PACS-2. A peak maximum was observed at

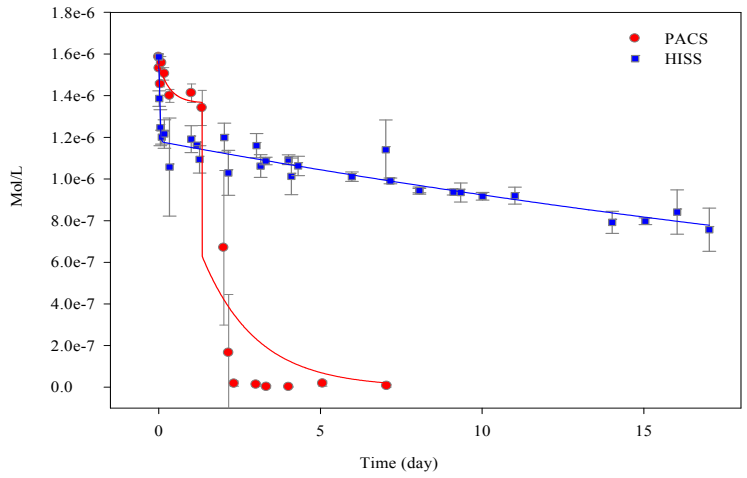

A

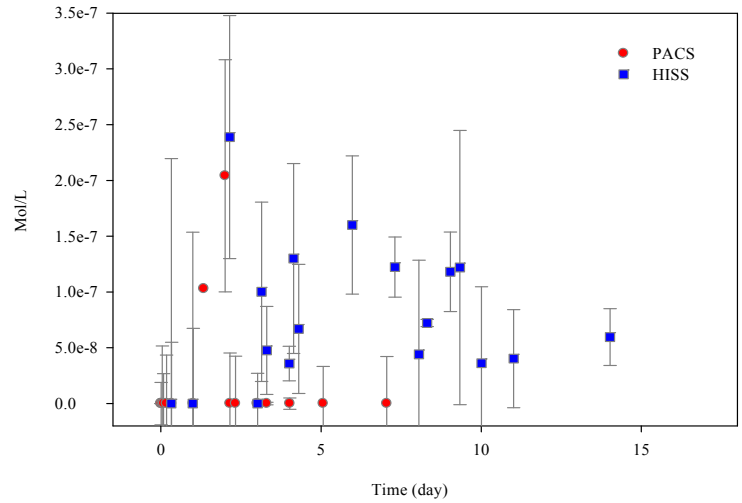

B

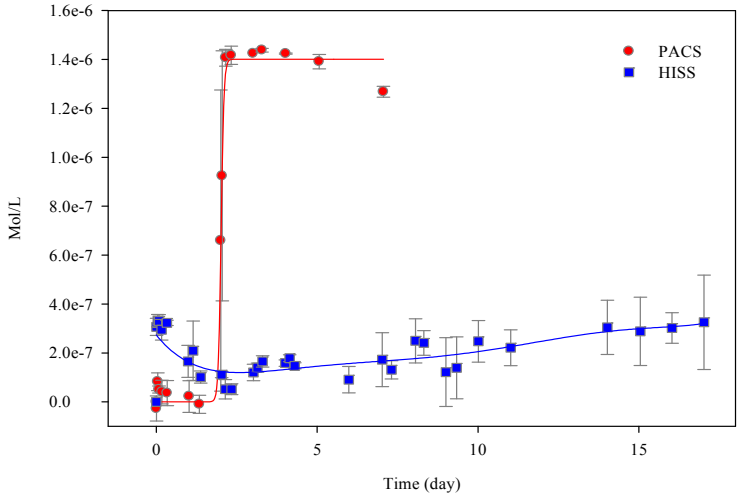

C

Figure 3.16. Naphthalene distribution kinetic curves for PACS-2 and HISS-1 slurries. **(A)** naphthalene dissolved**. (B)** naphthalene labile sorbed, **(C)** naphthalene bound residue. Initial naphthalene concentration 1.6×10^{-6} M at 25.0°C. **(A)** curves fitted using exponential decay, **(B)** free hand curve fitted, **(C)** curves fitted using least square regression.

day 2 of the time-dependent concentration curve of the labile sorbed naphthalene of the naphthalene-spiked PACS-2 slurries. In contrast to the PACS-2 system, a relatively constant amount of labile sorbed naphthalene that oscillated between $0.7x10^{-7}$ to $1.6x10^{-7}$ M was observed with HISS-1 sediment. The naphthalene concentration in the bound residue fraction for HISS-1 showed a constant increase over time, reaching a final concentration of $3x10^{-7}$ M. This concentration is one order of magnitude smaller than the concentration found in the case of PACS-2 (i.e., $1.4x10^{-6}$ M).

In agreement with literature[6-8,12,20,22,64] the sorption of naphthalene was more favorable in the case of the sediment with higher carbon content, i.e., with PACS-2. Naphthalene sorbed was mainly retained as a bound residue in the case of PACS-2, whereas in the case of HISS-1 naphthalene sorbed was approximately distributed in a 1:2 ratio between the labile sorbed and bound residue fractions, respectively.

The sorption mechanism must be clearly different between these two sediments. At the same initial naphthalene concentration ($1.6x10^{-6}$ M), naphthalene sorbed completely onto the PACS-2 sediment in less than three days, whereas HISS-1 was still uptaking naphthalene from solution at day 17.

Several authors had reported the influence of natural organic matter content on the sorption of hydrophobic aromatic compounds onto soils and sediments.[12,64,65] Huang and Weber[65] found that sorption and desorption processes depend not only on the quantity of organic matter present in the solid, but also on the quality of the organic matter. By comparing the sorption of phenanthrene in several soils, they could relate the composition of the organic matter, in terms of the oxygen to carbon (O/C) ratio, to the fraction of sorbed phenanthrene. It was found that a reduction in the oxygen to carbon (O/C) ratio caused an increase on the amount of sediment-bound phenanthrene. Xing[12] obtained

similar results for the sorption of naphthalene onto soils. In this case, Xing correlated the aromaticity of the natural organic matter to the sorption of the hydrophobic organic compound. Naphthalene uptake was favored in soils that had more aromatic content than those that were rich in aliphatic chains, thus young soils demonstrated lower sorption capacity compare to older soils.

3.3.4.3 Sorption - Desorption Comparison

Comparison between the total amount of naphthalene released at the end of the desorption process with the concentration of naphthalene bound residue shows that a considerable fraction of naphthalene remains bound to the sediment. For example, in the case of PACS-2 slurries with an initial naphthalene concentration of $1.6x10^{-6}$ M, the dissolved naphthalene concentration after seven days of desorption reached a concentration of $0.1x10^{-6}$ M whereas the naphthalene bound residue concentration reached $1.3x10^{-6}$ mol/L. The amount of naphthalene that remained as a bound residue was one order of magnitude bigger than the amount of dissolved naphthalene after 7 days of desorption. In the case of HISS-1, the dissolved naphthalene concentration at day 10 was $0.8x10^{-7}$ M, which is four times smaller than the bound residue concentration of $3.2x10^{-7}$ M. Increasing the initial naphthalene concentration in PACS-2 slurries changes drastically the ratio of dissolved naphthalene to bound residue naphthalene. At an initial naphthalene concentration of $4.0x10^{-6}$ M, the dissolved naphthalene concentration obtained after seven days of desorption was $0.2x10^{-6}$ mol/L whereas the concentration of naphthalene bound residue was in the order of $0.6x10^{-6}$ mol/L. In this case, the bound residue concentration is only three times bigger than the concentration of dissolved naphthalene. This suggests that a significant fraction of the $2.4x10^{-6}$ M naphthalene

(concentration difference between $1.6x10^{-6}$ and $4.0x10^{-6}$ M) was weakly bound to the sediment and can be released to solution in a relatively short time.

The above-mentioned results illustrate the differences between the sorption and desorption mechanism. From a mechanistic point of view the overall sorption and desorption processes are different, but when comparing the rate coefficient for the slow sorption process with the rate coefficient of the desorption process, no significant differences were found. The average rate coefficient for the slow sorption process in the case of PACS-2 spiked with $1.6x10^{-6}$ M or $4.0x10^{-6}$ M naphthalene was 0.6 ± 0.0 day^{-1} in both cases. This is comparable with the average rate coefficient of 0.5 ± 0.1 day^{-1} determined for the desorption process having same initial naphthalene concentration. These results are similar to those reported by Karickhoff[16] during the sorption/desorption of naphthalene onto sediments. He found that there were no significant differences between the slow sorption and the desorption rate coefficients. His desorption rate coefficient was smaller by a factor of 2 compared to the sorption rate coefficient.[16] In the case of HISS-1, the rate coefficients of the slow sorption and desorption rate coefficients were different and did not follow the same trend as observed with PACS-2. The rate of sorption was more than one order of magnitude smaller than the desorption rate. This probably indicates that the chemical and physical composition of the sediment used by Karickhoff was similar to the PACS-2 sediment.

There are several theories that explain the formation and existence of the bound residue or resistant fraction.[9,66] Kan and collaborators[66] explained the formation of this resistant fraction due to physical-chemical rearrangements in the solid phase after sorption has occurred, thus changing the molecular environment from which desorption would take place. Consequently, the desorption process takes place from different

sorption sites from those that existed during the sorption process. These two processes are therefore considered to be irreversible and, the solute that remains bound to the solid is considered to be in the irreversible compartment. This irreversible compartment has a maximum capacity and can be filled in a stepwise fashion in multiple sorption/desorption steps.[9,66] Also, the bound residue fraction has been explained as a consequence of the analyte sorption onto heterogeneous sorption sites that have high sorption energy and specificity. These characteristics are attributed to fundamental differences in the organic matter to which the hydrophobic organic compounds are sorbed.[23,66,67] The resistant fraction has also been explained as occurring due to the differences in the sorption and desorption rates. Connaughton and collaborators[31] modeled the bound residue formation as a series of rate-limiting compartments. They indicated that the desorption from labile surface sites would be relatively faster compare to the desorption from non-labile sorption sites, thus desorption from the bound residue fraction would be the rate determining step in the overall sorption-desorption process.[68]

3.3.4.4 Generalization of Sorption / Desorption Processes (Model)

A general description of the sorption-desorption kinetic will be given below.

From the naphthalene-spiked PACS-2 slurries at C_0 equal to $1.6x10^{-6}$ M, the disappearance of the labile sorbed fraction coincides with the formation of the bound residue. The maximum labile sorbed fraction attained at day 2 was seven times smaller than the fraction of bound residue for the same day. The bound residue fraction was 99% of the total naphthalene concentration.

In the case of naphthalene-spiked PACS-2 slurries at C_0 equal to $4.0x10^{-6}$ M, there is not correlation between the formation of the labile-bound and bound residue fractions.

The naphthalene bound residue was observed at the onset of the sorption experiment whereas the naphthalene labile sorbed fraction reached a maximum at day 3. In general the labile fraction formed was two times smaller than the bound residue fraction. The first rate coefficient (92 day^{-1}) for the sorption process at C_0 equal to $4.0x10^{-6}$ M is large compared to first rate coefficient (3 day^{-1}) for the sorption process at C_0 equal to $1.6x10^{-6}$ M. Therefore, contrary to what was observed, the labile sorbed fraction should have appeared earlier if the first rate coefficient of 92 day^{-1} is associated with the rate of formation of the labile sorbed fraction.

For the naphthalene-spiked PACS-2 slurries with C_0 equal to 7.8 $x10^{-6}$ M, the formation of the labile sorbed and bound residue fractions is also not correlated. In this case, between day 2 and 3 the labile fraction was 50% smaller than the bound residue. This situation changed completely between day 10 to 17 whereby the labile fraction became greater than the bound residue by 1.7 times. The first rate coefficient (84 d^{-1}) for the sorption process at C_0 equal to $7.8x10^{-6}$ M is comparable to first rate coefficient (92 d^{-1}) for the sorption process at C_0 equal to $4.0x10^{-6}$ M. In this case, the labile sorbed fraction appeared immediately at the onset of the sorption experiment as expected.

The fact that the first sorption rate coefficient at C_0 equal to 1.6 $x10^{-6}$ M is smaller than the first sorption rate coefficient at the other two C_0 systems means that sorption proceeded via a different mechanism at C_0 equal to 1.6 $x10^{-6}$ M compare to the other two systems. The sorption rate coefficient of a true first order sorption process would be independent from the magnitude of C_0. This is obviously not the case here, thus the possibility that a second order reaction, which would depend on, the initial concentration of naphthalene would need to be investigated in the future.

In the case of naphthalene-spiked HISS-1 slurries with C_0 equal to 1.6 $x10^{-6}$ M, there is a rapid formation of the bound residue during the first day, which then decreases to a minimum at day 2. No correlation between the formation of the bound residue and the labile sorbed fraction was observed. This suggests that the kinetics of the two processes is independent and uncorrelated.

The initial two-box model (see Equation 1.7) in which the sorption of naphthalene was considered to occur as a two-step process seems to be operational for the system with C_0 equal to $1.6x10^{-6}$ M and $7.8x10^{-6}$ M but inconsistent with the system with C_0 equal to $4.0x10^{-6}$ M. The sorption process seems to operate according to the following linked chemical equation:

$$\text{Dissolved} \xrightarrow{k_1} \text{labile sorbed} \xrightarrow{k_2} \text{Bound residue}$$

When k_1 (the first measured rate coefficient) is greater than k_2 (the second measured rate coefficient) as in the case of C_0 equal to 1.6 $x10^{-6}$ M and $7.8x10^{-6}$ M, the labile fraction will appear first follow by the formation of the bound residue. This should be considered as a preliminary model since it does not account for the results obtained when C_0 equal to 4.0 $x10^{-6}$ M.

The desorption process seems to operate in a one step process as follows since little difference was observed between the offline and online HPLC kinetic curves:

$$\text{Bound Residue} \xrightarrow{k_{-2}} \text{Dissolved}$$

The measured desorption rate coefficient (approximately 0.5 day^{-1}) at C_0 equal to 1.6 $x10^{-6}$ M and $4.0x10^{-6}$ M is consistent with the slow disappearance of dissolved naphthalene as shown by the second rate coefficient (0.6 day^{-1}). This slow disappearance or recovery of dissolved naphthalene is consistent with the existence of a fraction of naphthalene bound residue. The above preliminary sorption-desorption model will need to be tested under similar experimental conditions as in this study using different geosorbents-PAH systems in order to be confirmed.

CONCLUSIONS

An online microextraction and offline centrifugation HPLC methodologies were adapted to study the sorption kinetics of PAHs in geosorbents. These methodologies allowed the quantification of sorbed and free naphthalene. Using the online microextraction and offline centrifugation HPLC, it was possible to differentiate between the "degree of sorption", i.e., species that were labile sorbed (easy to remove) and species that remained strongly sorbed onto the solid (bound residue fraction). This differentiation between sorbed species represents an important advantage over other traditional experimental techniques that require intense labor and great investment of time to deliver the same or lower-quality kinetic results.

An extreme case of a volatile PAH compound (i.e., naphthalene), in contact with low carbon content quartz-like marine sediment and with moderately high carbon content quartz-like marine sediment was evaluated. These are limiting cases for the utilization of the online microextraction and offline centrifugation HPLC methodologies. Distribution of naphthalene between the free and sorbed states was quantified and the distribution kinetics was followed. As well, the desorption process between naphthalene and the test sediments were investigated.

A preliminary sorption-desorption model that consists of a two-step sorption process and a one step desorption process is proposed.

SUGGESTIONS FOR FUTURE RESEARCH

The determination of the sorption capacity for the naphthalene-marine sediments systems investigated in this study is required to fully characterize and model the kinetics and equilibrium behavior of naphthalene in contact with PACS-2 and HISS-1 sediments.

The sorption-desorption kinetics study should be applied to the homologous series of PAH with various quartz-containing sediments and with varying organic carbon content. This would allow the building up of a database that comprises kinetic rate coefficients, labile sorption capacities, and equilibrium constants. This information can be used to improve computational predictive calculations that could be used, for example, to forecast endpoints of a cleaning process. This database could provide enough information to examine the effects that chemical composition of sorbate particles have on the sorption of PAHs and, would provide time-dependent distributions of the PAHs between free and sorbed states in a real environmental system.

Identification of the chemical nature of the unknown chromatographic signal needs to be investigated. Its role in the sorption-desorption of naphthalene in contact with marine sediments needs to be clarified.

The adapted online and offline HPLC techniques can still be improved. For example the use of spinning bars to keep a uniform distribution of solids in the slurry needs to be reconsidered. It is important to verify the incidence of its use in the sorption – desorption processes due to the possibility of abrasion and changes in the morphology of the solid. It will be also important to assess the impact that pre-treatment of the solid samples can have on the chemical and physical integrity of the solid. In particular, storage and rewetting procedures should be investigated. Finally, the use of co-solvents

to increase the analyte solubility in the sediment slurries should be studied in terms of their persistence in solution and, consequently, of their potential impact on the total organic carbon content in the slurries.

REFERENCES

1. Neff J.M. *Polycyclic Aromatic Hydrocarbons in the Aquatic Environment. Sources, Fates and Biological Effects*. Applied Science Publishers Ltd. London 1979.

2. Andrews R. *Environ. Sci. Technol*., **1995**, 29,11.

3. Vo-Dinh T. In *Chemical Analysis of Polycyclic Aromatic Compounds*; Winefordner J. Ed.; New York 1984; Vol. 101, Chapter 1.

4. Li, J., Langford, C., and Gamble, D. *J. Agric. Food Chem.,* **1996**, 44, 3672-3679.

5. Jonker, M., and Koelmans, A., *Environ. Sci. Technol*., **2002**, 36,3725 – 3734.

6. Hassett J. and Banwart W. In *Reactions and Movement of Organic Compounds in Soil*; Sawhney, B.L., Brown, K., Eds; Soil Science Society of America: Madison, WI, 1989; Chapter 2, pp 31-43.

7. Pignatello, J.J. In *Reactions and Movement of Organic Compounds in Soil,* Sawhney, B.L., Brown, K., Eds. Soil Science Society of America, Madison, WI, 1989; Chapter 3, pp 45-80.

8. Means, J.C., Wood, S.G., Hasset, J.J., and Banwart, W.L. *Environ. Sci. Technol*., **1980**,14, 1524 – 1528.

9. Kan, A.T., Fu, G., and Thomson, M.B. *Environ. Sci. Tech*., **1994**, 28, 859-867.

10. Chiou, C. In *Reactions and Movement of Organic Compounds in Soil,* Sawhney, B.L., Brown, K., Eds; Soil Science Society of America: Madison, WI, 1989; Chapter 1, pp 1-29.

11. VanLoon, G., and Duffy, S.J. *Environmental Chemistry. A Global Perspective*, Oxford Eds.; pp 300-317

12. Xing, B. *Chemosphere*, **1997**, 35, 633 – 642.

13. Karickhoff, S.W., Brown, D.S., and Scott, T. A., *Water Research*, **1979**, 13, 241-248.

14. Murphy, E. M., Zachara, J. M., and Smith, S.S. *Environ. Sci. Technol*., **1990**,24, 1507 - 1516.

15. Kollist-Siigur, K., Nielsen, T., Gron, C., Hansen, P., Helweg, C., Jonassen, K., Jorgensen O., and, Kirso U., *J. Environ. Qual*., **2001**, 30, 526 - 537.

16. Karickhoff, S.W., In *Contaminants and Sediments*, Baker, R.A., Ed.; Ann Arbor Science Publishers: Ann Arbor, MI, 1980; pp 193-205.

17. Mader, B.T., Uwe-Goss, K., and Eisenreich, S.J. *Environ. Sci. Technol*., **1997**,13, 1079 - 1086.

18. Zeielke, R.C., Pinnavaia, T.J., and Mortland, M.M. In *Reactions and Movement of Organic Compounds in Soil*, Sawhney, B.L., Brown, K., Eds; Soil Science Society of America: Madison, WI, 1989; Chapter 4, pp 81-97.

19. Ghosh, D.R., and Keinath, T. M., *Environ. Progress*, **1994**,13, 51-57.

20. Luthy, R., Aiken, G. R., Brusseau, M.L., Cunningham, S.D., Gschwend, P.M., Pignatello, J.J., Reinhard, M., Traina, S.J., Weber, W. J. and Westall, J.C. *Environ. Sci. Technol*., **1997**, 31, 3341-3347.

21. Wu, S., and Gschwend, P.M. *Environ. Sci. Technol*., **1986**, 20, 717-725.

22. Karickhoff, S.W., and Morris, K.R., *Environ. Toxicol. Chem.*, **1985**, 4, 469-479.

23. Ghosh, U., Gillette S., Luthy, R., and Zare R. *Environ. Sci. Technol*., **2000**, 34, 1729-1736.

24. Brusseau, M. L., Jessup, R.E., and Rao, P. S. *Environ. Sci. Technol*., **1990**,24, 727 - 735.

25. Gamble, D., Bruccolleri, A., Lindsay, E., Langford, C., and Leyes, G. *Environ. Sci. Technol*., **2000**, 34, 125-129.

26. Gamble, D., Bruccolleri, A., Lindsay, E., Langford, C., and Leyes, G. *Environ. Sci. Technol*., **2000**, 34, 120-124.

27. Gamble, D., Lindsay, E., Bruccolleri, A., Langford, C., and Leyes, G. *Environ. Sci. Technol*., **2001**, 35, 2375-2380.

28. Gamble, D., and Khan, S. *J. Agric. Food Chem.,* **1990**, 38, 297-308.

29. Gamble, D., Langford, C., and Webster, B. G. R. *Reviews Environ. Contam. Toxicol.*, **1994**, 135, 63 - 91.

30. Huang, W., and Weber, W.J. *Environ. Sci. Technol*., **1997**, 31, 3238 – 3243.

31. Connaughton, D. F., Stedinger, J.R., Lion, L.W., and Shuler M. *Environ. Sci. Technol*., **1993**, 27, 2397 – 2403.

32. Carmichael, L.M., Christman, R.F., and Pfaender, F.K. *Environ. Sci. Technol.* **1997**, 31,126-132.

33. Weber, W., McGinley, P., and Katz, L.F. *Environ. Sci. Technol*., **1992**, 26, 1955-1962.

34. Gamble, D., and Khan, S. *Can. J. Chem.* **1992**, 70, 1597-1603.

35. Sparks, D. *Kinetics of Soil Processes*; Academic: San Diego, 1989; Chapter 3.

36. Young, T. M. and Weber, W.J. *Environ. Sci. Technol*., **1995**, 29,92-97.

37. Lam, M. T., Gamble, D. S., Chakrabarti, C. L. and, Ismaily, A. L., *Int. J. Environ. Anal. Chem*., **1996**, 64, 217-231

38. Gamble, D.S., and Ismaily, L.A. *Can. J. Chem*., **1992**,70, 1590-1596.

39. Gamble D S., Schnitzer, M. and, Kerndorff H., *Geochimica et Cosmochimica Acta*., **1983**, 47, 1311-1323.

40. Sewell, P. A., and Clarke, B. *Chromatographic Separations*. Kealey, D. Ed. J. Wiley. London 1987, pp 85-88.

41. Strobel, H.A., and Heineman, W.R. *Chemical Instrumentation: A systematic Approach.* J. Wiley. Canada 1989, pp 373-377.

42. Belliveau, S. M., Henshelwood, T. L., and Langford, C.H., *Environ. Sci. Technol*., **2000**, 34, 2439-2445.

43. Federal register 1 Parts 260-299, Environmental Protection Agency, 1996.

44. Piatt, J., Backhus, D., Capel, P., and Eisenreich, S. *Environ. Sci. Technol*. **1996**, 30, 751-760.

45. Schwarzenbach, R., Gschwend, P., and Imboden, D. *Environmental Organic Chemistry*. Second Ed., Wiley-Interscience, N.J., **2003,** pp.387-448.

46. *HISS-1, MESS-3, PACS-2 Marine Sediment Reference Materials for Trace Metals and other Constituents.* National Research Council of Canada Institute for National Measurement Standards, 2000.

47. Sheldrick B. H *Analytical Methods Manual.* Land Resource Research Institute 84-001 file. 1984. Retrieved from: http://sis.agr.gc.ca/cansis/publications/manuals/analytical.html, on August 11 2001.

48. Gartley K.L. *Recommended Soluble Salts Tests.* The State University of New Jersey Rutgers, pp 70-75, 1994.

49. *Organic Application Note CNS 2000*, Form No. 203-821-170, LECO Corporation, 2000.

50. Northcott, G. L. and Jones, K.C. *Environ. Toxicol. Chem.*, **2000**,19, 2418-2430.

51. Northcott, G. L. and Jones, K.C. *Environ. Toxicol. Chem.*, **2000**,19, 2409-2417.

52. Gilchrist, G., Gamble, D., Kodama, H., and Khan, S. *J. Agric. Food Chem*. **1993**, 41, 1748-1755.

53. Ball W.P. and Roberts P.V. *Environ. Sci. Technol*. **1991**, 25, 1237-1249.

54. Ogwada, R.A. and Sparks D.L. Soil, *Sci. Soc. Am. J.* **1986**, 50, 1158-1162.

55. Johnson, M. D., Keinath M. and Weber W.J. *Environ. Sci. Technol*. **2001**, 35, 1688-1695.

56. Chen, W. Kan A., Fu Gongmin F., and Tomson M.B. *Environ. Toxicol. Chem.*, **2000**,19, 2401-2408.

57. Northcott, G. L. and Jones, K.C. *Environ. Sci. Technol*. **2001**, 35, 1103-1110.

58. Northcott, G. L. and Jones, K.C. *Environ. Sci. Technol*. **2001**, 35, 1111-1117.

59. White J., and Pignatello J.J. *Environ. Sci. Technol*. **1999**, 33, 4292-4298.

60. Zhao D., Pignatello J.J., White J.C. Braida W., Ferrandino F. *Water Resour. Res.*, **2001,**37,2206-2212.

61. Brusseau M., Larsen T., and Christensen T. *Water Resour. Res.*, **1991,**27,1137-1145.

62. Rosenberg, E., Krska, R., Wissiack, R., Kmetov, V., Josephs, R., Razzazi, E. and Grasserbauer, M. *J. Chromatogr. A.* **1998**, 819, 277 - 288.

63. Anacleto, J. F., Ramaley, L., Benoit, F. M., Boyd, R. and Quilliam, M. A. *Anal. Chem.* **1995**, 67, 4145 - 4154.

64. Kukkonen J.V., Landrum P.F. Mitra S., Gossiaux D., Gunsarsson J. and Weston D., *Environ. Sci. Technol*. **2003**,27,4656-4663.

65. Huang, W., and Weber, W.J. *Environ. Sci. Technol*., **1997**,31, 2562-2568

66. Kan, A.T., Fu, G., Hunter M., Chen W., Ward C.H. and Thomson, M.B. *Environ. Sci. Tech*., **1998**, 32, 892-902.

67. Talley, J. W., Ghosh U., Tucker S., Furey J.S. and Luthy R. G. *Environ. Sci. Tech*., **2002**, 36, 477-483.

68. Huang, W., H., Yu, and W. Weber, *Journal of Contaminant Hydrology*, **1998**, 31, 129-148.

APPENDICES

Appendix 1. Syringe filter membranes tested for phase separation of slurries.

Membrane Material	Pore Size (μm) x Diameter (mm)	Supplier
Nylon Cameo 3N	0.22 x 3.0	Micron Separations
Polytetrafluorethylene (PTFE)	0.2 x 4.0	Millipore
Polyvinylidene difluoride (PVDF)	0.2 x 4.0	Millipore
Cameo Cellulose Acetate	0.2 x 13	Whatman
Polypro-hydrophilic Polypropylene	0.2 x 13	Whatman
Glass micro Fiber GD/X	0.45 x 13	Whatman
Glass micro Fiber GF/F	0.7 x 13	Whatman

Appendix 2. Comparison of chromatographic peak areas using Student's t-test. Losses of naphthalene by evaporation to headspace for spiked slurries and standard solutions.

Hypothesis

There are no significant differences, at 95% confidence level, between the average naphthalene concentrations in headspace of spiked slurries and standard solutions.

Procedure

Duplicate mixing vials for naphthalene standard solutions and naphthalene-spiked slurries, both at 0.5 mg/L were prepared. The initial volume in all cases was 28 mL. A blank solution (2% acetonitrile) was also prepared to correct the chromatographic signals for matrix background. Uptake of 0.15 mL aliquots was performed to complete a total of 20 in 15 days. Total volume retrieved from each vial was in all cases 3 mL. After this period of time, analysis of naphthalene present in headspace was performed using GC-FID. Triplicate analysis of each vial was performed by manual injection of 500 μL of gas from headspace.

Statistic Analysis

$$t_{Calculated} = \frac{X_{1\ average} - X_{2\ average} * SQT(n_1 * n_2 / n_1 + n_2)}{S_{pooled}}$$

$$S_{pooled} = SQT(s_1^{\wedge 2} * (n_1 - 1) + s_2^{\wedge 2} * (n_2 - 1) / (n_1 + n_2 - 2))$$

If $t_{calculated} > t_{tabulated}$ at 95% confidence level, then the two means are statistically different

Results

	Standard Solution		Spiked Slurries	
	Series 1 Area (Counts)	Series 2 Area (Counts)	Series 1 Area (Counts)	Series 2 Area (Counts)
1	1497	1379	1220	1290
2	1647	1404	1310	1257
3	1437	1403	1241	1318
Average, X	**1527**	**1396**	**1257**	**1289**
Standard error,s	**108**	**14**	**47**	**31**
RSD (%)	**7**	**1**	**4**	**2**
Data points, n	3	3	3	3

There were no statistical differences, at 95% confidence level, between the concentration of naphthalene present in headspace of standard solutions and spiked slurries.

Appendix 3. HPLC-APCI-MS conditions for the analysis of unknown compound in the liquid phase of naphthalene-spiked slurries, naphthalene standard solutions and blank solutions.

Chromatographic conditions	
Column	5μm x 4.6mm i.d.x150mm. Eclipse XD8C_8
Mobile phase	Acetonitrile 80%/ Water 20% Isocratic elution
Flow rate	1.0 mL/min
Column temperature	25 °C
Injection volume	20 μL

MS conditions			
Mode			
Source	APCI	Divert valve	To source
Ionization mode	Positive	Target	30000
Scan range	50-600 m/z	Max. Accumulation Time	50.00 ms
Scan resolution	13.000 m/z/s		
Step size	0.1 amu		
Peak width	0.1 min		
Tune Page			
Voltage capillary	+4000 V	Drying gas flow	6 L/min
End plate offset	-500 V	Drying gas temperature	350 °C
Corona current	-5000 nA	APCI temperature	500 °C
Nebulizer	60 psig		
Expert Parameter Settings			
Skim 1	-20.1 V	Skim 2	-6.0 V
Cap exit offset	-93.4 V	Cap exit	-88.3 V
Octapole	-1.51 V	Octapole RF	118.9 V
Octapole delta	-2.22 V	Lens 1	-5.0 V
Trap drive	38.7	Lens 2	-60.0 V